ESAIM: M2AN 45 (2011) 277–307
DOI: 10.1051/m2an/2010042

ESAIM: Mathematical Modelling and Numerical Analysis
www.esaim-m2an.org

ENABLING NUMERICAL ACCURACY OF NAVIER-STOKES-α THROUGH DECONVOLUTION AND ENHANCED STABILITY*

Carolina C. Manica[1], Monika Neda[2], Maxim Olshanskii[3] and Leo G. Rebholz[4]

Abstract. We propose and analyze a finite element method for approximating solutions to the Navier-Stokes-alpha model (NS-α) that utilizes approximate deconvolution and a modified grad-div stabilization and greatly improves accuracy in simulations. Standard finite element schemes for NS-α suffer from two major sources of error if their solutions are considered approximations to true fluid flow: (1) the consistency error arising from filtering; and (2) the dramatic effect of the large pressure error on the velocity error that arises from the (necessary) use of the rotational form nonlinearity. The proposed scheme "fixes" these two numerical issues through the combined use of a modified grad-div stabilization that acts in both the momentum and filter equations, and an adapted approximate deconvolution technique designed to work with the altered filter. We prove the scheme is stable, optimally convergent, and the effect of the pressure error on the velocity error is significantly reduced. Several numerical experiments are given that demonstrate the effectiveness of the method.

Mathematics Subject Classification. 65M12, 65M60, 76D05.

Received May 4, 2009. Revised October 29, 2009 and March 29, 2010.
Published online August 2, 2010.

1. Introduction

We study a finite element method (FEM) for the NS-α model that employs both a stabilization of grad-div type and adapted van Cittert approximate deconvolution to produce high accuracy flow simulations. This new scheme provides accurate computations with NS-α, which is widely known as a *physically* accurate model, but whose widespread use has not yet caught on due to large error in its numerical approximations. Motivated by the belief that the large errors are a shortcoming of the FEM implementations and not the model, we identify two major sources of numerical error arising in FEM discretizations of NS-α, and propose a scheme that "fixes" both

Keywords and phrases. NS-alpha, grad-div stabilization, turbulence, approximate deconvolution.

* *M. Olshanskii was partially supported by the RAS program "Contemporary problems of theoretical mathematics" through the project No. 01.2.00104588 and RFBR Grant 08-01-00415 and L.G. Rebholz was partially supported by NSF grant DMS0914478.*

[1] Departmento de Matemática Pura e Aplicada, Universidade Federal do Rio Grande do Sul, Brazil. carolina.manica@ufrgs.br; http://chasqueweb.ufrgs.br/~carolina.manica

[2] Department of Mathematics, University of Nevada, Las Vegas, USA. Monika.Neda@unlv.edu; http://www.pitt.edu/~mon5

[3] Department of Mechanics and Mathematics, Moscow State M. V. Lomonosov University, Moscow 119899, Russia. Maxim.Olshanskii@mtu-net.ru; http://www.mathcs.emory.edu/~molshan

[4] Department of Mathematical Sciences, Clemson University, Clemson, SC 29634, USA. rebholz@clemson.edu; http://www.math.clemson.edu/~rebholz

Article published by EDP Sciences

© EDP Sciences, SMAI 2010

https://doi.org/10.1051/m2an/2010042 Published online by Cambridge University Press

of them. Analysis of this new scheme shows both unconditional stability and optimal convergence, and several numerical experiments including the Green-Taylor vortex problem, flow over a step, and the 3d Ethier-Steinman problem demonstrate its effectiveness.

Originally called the 3d viscous Camassa-Holm equations [9], NS-α has attracted significant attention in recent years due to its many attractive mathematical and physical properties. It admits unique regular solutions [20, 37], is frame invariant [24], conserves energy, helicity, and 2d enstrophy [19,46], obeys Kelvin's circulation theorem [19], cascades energy through the inertial range at the same rate as the Navier-Stokes equations (NSE) up to a filtering radius dependent cut-off length scale after which it accelerates energy decay [19], can be fully resolved with $O(Re^{3/2})$ degrees of freedom (compared to $O(Re^{9/4})$ for the NSE) [19], and dissipates energy and helicity independent of Reynolds number as $O(U^3/L)$ and $O(U^3/L^2)$ respectively, as in true fluid flow [35].

These properties suggest NS-α is more *physically* accurate than many other models. For example, the $k-\epsilon$, Smagorinsky, Leray, and Bardina models do not conserve helicity and thus will nonphysically inject or dissipate helicity (and thus rotation) in their solutions. Moreover, the Bardina model [4,45] does not even conserve energy, the Leray model is not frame invariant and fails to satisfy Kelvin's circulation theorem [24], and the Smagorinksy model has been shown to dissipate energy too quickly through the inertial range [41]. However, despite all of NS-α's excellent theoretical properties, and that direct numerical simulation (DNS) testing of the model was successful for flow in a channel and in a cylinder [10–12,36], its use has still remained limited. We believe this has not been due to a lack of effort from the CFD (computational fluid dynamics) community or that the model itself is inherently inaccurate, but instead because of poor accuracy caused by subtle numerical problems arising in FEM implementations of the model.

NS-α uses the Helmholtz filter (also called the α filter), which for a chosen filtering radius α, is given by

$$\overline{u} := F\,u := (-\alpha^2\Delta + I)^{-1}u. \tag{1.1}$$

The NS-α model is then defined to be

$$\begin{aligned} u_t - \overline{u}\times(\nabla\times u) + \nabla p - \nu\Delta u &= f, &(1.2)\\ \nabla\cdot u = \nabla\cdot\overline{u} &= 0, &(1.3)\end{aligned}$$

with ν representing the kinematic viscosity.

Although (1.1)–(1.3) is well-posed in the periodic case, for wall bounded flows it is not. In this case, the divergence free condition $\nabla\cdot\overline{u}=0$ is not consistent with the definition of the filter in (1.1), which would have a unique solution without the constraint. However, this constraint is necessary for nonlinear stability (and thus well-posedness) of the system, so it cannot be removed. Hence the natural solution, first suggested in [47] and subsequently used successfully in [16,39], is to relax the filter equation with a Lagrange multiplier to allow for the divergence free constraint on the filtered velocity. This is accomplished by adding $0=\nabla(\nabla\cdot\overline{u})$ to the filter equation, then replacing $\nabla\cdot\overline{u}$ with the new variable (Lagrange multiplier) λ. Note this formulation has the additional advantage that the physically important constraint $\nabla\cdot u=0$ can now also be included. That this new system is well-posed now follows easily by the Galerkin method, essentially following proof by [20] for the periodic case. Hence the system we study is (1.2)–(1.3) with the filter equation

$$\overline{u} - \alpha^2\Delta\overline{u} + \nabla\lambda = u. \tag{1.4}$$

The scheme proposed herein attempts to reduce significantly the numerical error arising from two sources. First, the rotational form of the nonlinearity leads to a complex Bernoulli-like pressure. This Bernoulli pressure accounts for the kinematic term $\frac{u^2}{2}$ and so may share internal and boundary layers of the velocity field. Thus, if a mesh is not sufficiently fine a large pressure error arises, causing a scaling of the velocity error as *velocity error* $\approx$ *Re* * *pressure error* (*cf.* Sect. 4), where *Re* is the Reynolds number. Hence for large *Re*, the velocity error can be very large. In [33], it is shown that a similar problem arises when computing the Navier-Stokes equations (NSE) with the rotational form of the nonlinearity, and can be fixed with grad-div stabilization

https://doi.org/10.1051/m2an/2010042 Published online by Cambridge University Press

described in the next section. Similar fixes have been successfully used for the same purpose in the Stokes equations [43] and the steady NSE [42]. An extension of this idea to NS-α was proposed by Connors in [16], by adding the usual grad-div stabilization term to a standard FEM for NS-α. However, his analysis showed that for unconditional stability, the grad-div stabilization parameter needs chosen smaller than $O(\nu)$, which is far from an optimal choice of $O(1)$. We find that, by also adding grad-div stabilization to the filter equation with a carefully chosen coefficient, no condition needs placed on the grad-div stabilization parameter for unconditional stability, allowing for the optimal reduction of the effect of the pressure error on the velocity error. We refer to these two grad-div stabilizations as a modified grad-div stabilization, as they really work together as one stabilization, and with a single parameter, to reduce error in an unconditionally stable way.

We point out that the stabilization method suggested herein is inherently tied to Taylor-Hood type elements, that is, the (P_k, P_{k-1}) pair for $k \geq 2$. Although this is perhaps the most widely used element pair for finite element computations, it is not the only one. Other element choices may naturally lead to other stabilizations, or none at all, at least for the purpose of reducing the effect of the Bernoulli pressure. For example, Scott-Vogelius elements use a large enough pressure space (see [8] for a study of these elements with the Navier-Stokes equations) that such a stabilization term would be implicitly zero. Similarly, a local discontinuous Galerkin scheme has been developed in [14] that also would provide pointwise mass conservation. Another example of interesting element choice would be equal order elements with a pressure stabilization for stability, as in [7], since the increased degree of approximating polynomials for the pressure will alleviate some of the error arising from the Bernoulli pressure. Naturally, these alternate element choices have their drawbacks as well, and herein we consider only the Taylor-Hood type element. Still, future numerical studies of this model with such element choices would be interesting and likely worthwhile.

The second major source of error in NS-α computations (and in any α-type model) arises from the model's consistency error to the NSE. Even for smooth flows, it is clear from (1.3)–(1.4) that one cannot expect accuracy better than $O(\alpha^2)$ from the model itself, even before any computational error is introduced. It is typical to have $\alpha = O(h)$, where h is the mesh size. In the series of papers [1,2,49] Stolz, Adams and Kleiser suggested to reduce the filter-induced consistency error in turbulence models *via* the van Cittert method of approximate deconvolution and proved it to be an excellent tool for producing reduced order simulations with high accuracy. The method constructs a family D_N of approximate inverses to the filter F as the truncation of the nonconvergent power series: $F^{-1} = \sum_{n=0}^{\infty}(I-F)^n$:

$$D_N = \sum_{n=0}^{N}(I-F)^n. \tag{1.5}$$

In the NS-α model with approximate deconvolution of order N the filtered velocity $\overline{u}$ in (1.2) is modified as

$$\overline{u} \to D_N \overline{u}.$$

In [46], it is shown how van Cittert approximate deconvolution can be added to NS-α to increase its consistency error to the NSE to $O(\alpha^{2N+2})$, where N is typically chosen $1 \leq N \leq 5$. Computations in [47] show this can improve accuracy in simulations. This technique has also been used successfully to improve accuracy in simulations using other α-type models, such as Leray-α and NS-$\overline{\omega}$ [32,34,47]. For numerical experiments in this paper we set either $N = 0$ (no deconvolution) or $N = 1$.

The numerical examples presented herein will show that *the combination of modified grad-div stabilization with approximate deconvolution* has a tremendous impact in obtaining accurate solutions with FEM discretizations of NS-α. Although one rarely will know *a priori*, sometimes the velocity error will be dominated by the modeling error, and other times by ($Re *$ pressure error). By themselves, the proposed "fixes" of the scheme will help significantly in only one of the two cases, but likely very little in the other. When used together, however, they can greatly reduce the error in most problems, and have an even greater effect than either one used individually.

This paper is arranged as follows. Section 2 introduces notation and important general properties of the nonlinear term and finite element spaces. In particular, it introduces the semidiscrete scheme, new discrete operators and relevant properties of induced norms. These are rather technical, but simplify the stability

https://doi.org/10.1051/m2an/2010042 Published online by Cambridge University Press

and convergence proofs. Section 3 presents a full discretization of the scheme and its stability analysis, together with some preliminary results needed in Section 4, in which the convergence analysis is proven. Section 5 features numerical experiments that corroborate the convergence analysis of Section 4 and show that the scheme is able to predict expected physical behavior accurately.

2. The finite element scheme and preliminaries

Let $\Omega \subset \mathbb{R}^d$, $d = 2, 3$, be a polyhedral domain and τ_h be a regular discretization of Ω such that the inverse inequality holds. Let $(X_h, Q_h) \subset (X, Q) = (H_0^1(\Omega)^d, L_0^2(\Omega))$ be the velocity-pressure spaces satisfying the discrete inf-sup (or LBB) condition [25]. Denote by $(\cdot,\cdot)$ and $\|\cdot\|$ the $L^2(\Omega)$ inner product and norm, respectively. The space H^k represents the Sobolev space $W_k^2(\Omega)$ and $\|\cdot\|_k$ denotes the norm in H^k. For functions $v(x,t)$ defined on the entire time interval $(0,T)$, we define $(1 \le m < \infty)$

$$\|v\|_{\infty,k} := \operatorname*{ess\,sup}_{0<t<T} \|v(t,\cdot)\|_k, \qquad \text{and} \qquad \|v\|_{m,k} := \left(\int_0^T \|v(t,\cdot)\|_k^m \, \mathrm{d}t \right)^{1/m}.$$

All other norms and inner products will be labeled with subscripts.

We make use of the following approximation properties:

$$\begin{aligned} \inf_{v \in X_h} \|u - v\| &\le C h^{k+1} |u|_{k+1}, \quad u \in H^{k+1}(\Omega)^d, \\ \inf_{v \in X_h} \|u - v\|_1 &\le C h^{k} |u|_{k+1}, \quad u \in H^{k+1}(\Omega)^d, \\ \inf_{r \in Q_h} \|p - r\| &\le C h^{s+1} |p|_{s+1}, \quad p \in H^{s+1}(\Omega). \end{aligned} \tag{2.1}$$

Moreover, if $\nabla \cdot u = 0$, then in the first estimates from (2.1), the finite element space X_h can be replaced by its subspace [6]:

$$V_h := \{ v_h \in X_h \,|\, (\nabla \cdot v_h, q_h) = 0 \ \ \forall q_h \in Q_h \}.$$

2.1. The finite element scheme

The spatial discretization of (1.2)–(1.3) reads: Find $\{u_h(t), p_h(t)\} \in X_h \times Q_h \ \forall t \in (0,T]$ solving

$$\begin{aligned} \left(\frac{\partial u_h}{\partial t}, v_h \right) + \nu(\nabla u_h, \nabla v_h) - (D_N^h F_h u_h \times (\nabla \times u_h), v_h) - (p_h, \nabla \cdot v_h) + (q_h, \nabla \cdot u_h) \\ + \gamma(\nabla \cdot u_h, \nabla \cdot v_h) = (f, v_h), \qquad \forall \{v_h, q_h\} \in X_h \times Q_h, \quad \forall t \in (0,T]. \end{aligned} \tag{2.2}$$

A particular time discretization is not important for us at this moment and will be specified later. The discrete filter F_h and the discrete deconvolution operator D_N^h are defined below. If $\gamma > 0$ then the violation of the divergence constraint by the finite element solutions is additionally penalized; $\gamma = 0$ corresponds to the plain Galerkin method. Adding such a term is known as *the grad-div stabilization* and corresponds to adding the vanishing $-\gamma \nabla \mathrm{div} u$ term to the momentum equation (1.2). The convergence analysis in Section 4 recovers the stabilizing effect of the γ-term with respect to a possible poor pressure resolution.

Besides the stabilizing of the Bernoulli pressures discretizations and turbulence modelling, penalizing the divergence constraint is not a new idea. This term was part of the Petrov-Galerkin method (SUPG) in [18,26]. In practice this term is often omitted, and until recently it was not clear if it is needed for technical reasons of the analysis or played an important role in computations. The role of the grad-div stabilization was

https://doi.org/10.1051/m2an/2010042 Published online by Cambridge University Press

again emphasized in the recent studies of the (stabilized) finite element methods for incompressible flow problems, see [21,38,43,50], also in conjunction with the rotation form of nonlinearities in the Navier-Stokes equations [33,34,42] and variational multiscale turbulence modelling [27]. Its relation to the variational multiscale approach is revealed in [15,22,44].

In numerical experiments done with LBB-stable finite element discretizations and presented further in the paper, we show that the simple choice $\gamma = 1$ already leads to a dramatic improvement of accuracy compared to $\gamma = 0$. Although $\gamma = 1$ may not be an optimal choice, it is not the intention of this paper to find optimal parameter. It should be noted, however, that if the discretization provides better pressure approximation, as happens with stabilized equal-order FE, one may put less emphasis on the additional enforcement of the divergence free constraint and decrease γ accordingly. The Scott-Vogelius element [48] ultimately enforces the divergence free condition point-wise. In a more general setting, γ may vary in Ω from element to element and an optimal choice may depend on a particular flow problem, discretization, etc., see [44] for a detailed discussion.

It remains to define the discrete filter F_h and the discrete deconvolution operator D_N^h. We found that it is important in numerical implementations to force the divergence-free condition for the filtered function (similar observations can be found in [16,39,47]). Therefore, instead of the discrete Helmholtz type problem we are considering the following discrete Stokes type problem: For a chosen filtering radius $\alpha > 0$ and a given $u \in L^2(\Omega)$ define $F_h u = \overline{u}^h$ from

$$\alpha^2 \left((\nabla \overline{u}^h, \nabla v_h) + \frac{\gamma}{\nu} (\nabla \cdot \overline{u}^h, \nabla \cdot v_h) \right) - (\lambda_h, \nabla \cdot v_h) + (q_h, \nabla \cdot \overline{u}^h) + (\overline{u}^h, v_h) = (u, v_h), \quad \forall \{v_h, q_h\} \in X_h \times Q_h. \tag{2.3}$$

It is important for the analysis and accurate numerics that the discrete filter (2.3) is also stabilized with the grad-div term and the parameters ν and γ are taken the same as in (2.2). The Lagrange multiplier λ_h is never used further in calculations.

Finally, given the discrete filter F_h the discrete van Cittert approximate deconvolution D_N^h is defined through (1.5) with F replaced by F_h. As an example, the first few operators of the family are

$$\begin{aligned} D_0^h \phi &= \phi, \\ D_1^h \phi &= 2\phi - \overline{\phi}^h, \\ D_2^h \phi &= 3\phi - 3\overline{\phi}^h + \overline{\overline{\phi}^h}^h. \end{aligned}$$

Further in this paper we prove stability and error estimate for this stabilized discrete NS-α model with the approximate deconvolution. For this purpose we need some technical results formulated further in this section.

2.2. Grad-div modified Laplacian and filtering

For both readability and a smooth analysis, we believe it is useful to develop notation for a grad-div modified Laplacian and the modified filter defined in terms of this new Laplacian.

We begin by defining the grad-div modified discrete Laplacian operator acting on the space of discretely solenoidal functions V_h.

Definition 2.1 (modified Laplacian)**.** Given parameters $\gamma, \nu > 0$, define the grad-div modified discrete Laplacian $\widetilde{\Delta}_h : H^1(\Omega) \to V_h$ as the unique solution in V_h to

$$(\widetilde{\Delta}_h \phi, v) = -(\nabla \phi, \nabla v) - \frac{\gamma}{\nu} (\nabla \cdot \phi, \nabla \cdot v), \quad \forall v \in V_h. \tag{2.4}$$

For $\phi \in L^2(\Omega)$, $F_h \phi = \overline{\phi}^h$ from (2.3) can equivalently be defined as the unique solution in V_h to

$$-\alpha^2 (\widetilde{\Delta}_h \overline{\phi}^h, v) + (\overline{\phi}^h, v) = (\phi, v), \quad \forall v \in V_h. \tag{2.5}$$

https://doi.org/10.1051/m2an/2010042 Published online by Cambridge University Press

Thus, restricted on V_h the filter F_h has a well-defined inverse and can be written in the following compact way: $F_h := (-\alpha^2\widetilde{\Delta}_h + I)^{-1}$.

The following lemma provides some simple identities and inequalities that arise from the filter definitions. They will be of great importance in the later analysis.

Lemma 2.2. *For $\phi \in L^2(\Omega)$, we have that*

$$\|\overline{\phi}^h\|^2 + \alpha^2\|\nabla\overline{\phi}^h\|^2 + \frac{\alpha^2\gamma}{\nu}\|\nabla\cdot\overline{\phi}^h\|^2 = (\phi, \overline{\phi}^h), \tag{2.6}$$

$$\|\nabla\overline{\phi}^h\|^2 + \frac{\gamma}{\nu}\|\nabla\cdot\overline{\phi}^h\|^2 + \alpha^2\|\widetilde{\Delta}_h\overline{\phi}^h\|^2 = (\nabla\phi, \nabla\overline{\phi}^h) + \frac{\gamma}{\nu}(\nabla\cdot\phi, \nabla\cdot\overline{\phi}^h), \tag{2.7}$$

$$\|\overline{\phi}^h\| \le \|\phi\|, \tag{2.8}$$

$$\|I - F_h\| \le 1, \tag{2.9}$$

$$\|\nabla\overline{\phi}^h\|^2 + \frac{\gamma}{\nu}\|\nabla\cdot\overline{\phi}^h\|^2 + \alpha^2\|\widetilde{\Delta}_h\overline{\phi}^h\|^2 \le \|\nabla\phi\|^2 + \frac{\gamma}{\nu}\|\nabla\cdot\phi\|^2. \tag{2.10}$$

Proof. The first identity follows immediately from choosing $v = \overline{\phi}^h$ in (2.5). For the second identity, choose $v = -\widetilde{\Delta}_h\overline{\phi}^h$ in (2.5) to get

$$\alpha^2\|\widetilde{\Delta}_h\overline{\phi}^h\|^2 - (\overline{\phi}^h, \widetilde{\Delta}_h\overline{\phi}^h) = -(\phi, \widetilde{\Delta}_h\overline{\phi}^h).$$

Since $\widetilde{\Delta}_h\overline{\phi}^h \in V_h$, the result now follows the definition of the modified discrete Laplacian (2.4). The inequalities (2.8) and (2.10) are immediate consequences of (2.6) and (2.7) respectively, by applying Cauchy-Schwarz and Young's inequalities. The inequality (2.9) follows from (2.8), noting that F_h also denotes the modified Helmholtz filter. □

2.3. Natural energy and energy dissipation norms

The numerical scheme studied herein can be more easily analyzed in the following natural energy and energy dissipation norms.

Definition 2.3. We define the natural energy and energy dissipation norms for NS-α-deconvolution to be

$$\|\phi\|^2_{E;N} := (\phi, D_N^h\overline{\phi}^h), \tag{2.11}$$

$$\|\phi\|^2_{\epsilon;N} := -(\widetilde{\Delta}_h\phi, D_N^h\overline{\phi}^h). \tag{2.12}$$

Remark 2.4. In their continuous forms, for general α, these norms (and the natural norms of continuous NS-α-deconvolution [19,46]) are equivalent to the H^{-1} and L^2 norms, respectively, which is one degree less than is common for fluid flow schemes. However, provided the inverse inequality holds and the filtering radius is chosen as $\alpha = O(h)$ (as it should be for optimal accuracy with sufficient regularization [32,34]) on V_h, these discrete norms are equivalent to the L^2 and H^1 norms, respectively, *cf.* [39].

For the ease of analysis, it will be very helpful to have equivalence between the natural norms for varying orders of deconvolution N.

Lemma 2.5. *For $\phi \in V_h$ and for each natural number N, the energy norm defined by (2.11) is equivalent to the zeroth order energy norm defined by (2.11). That is,*

$$\|\phi\|_{E;0} \le \|\phi\|_{E;N} \le \sqrt{N}\|\phi\|_{E;0}. \tag{2.13}$$

For $\phi \in V_h$ and for each natural number N, the energy dissipation norm defined by (2.12) is equivalent to the zeroth order energy dissipation norm defined by (2.12). That is,

$$\|\phi\|_{\epsilon;0} \le \|\phi\|_{\epsilon;N} \le \sqrt{N}\|\phi\|_{\epsilon;0}. \tag{2.14}$$

https://doi.org/10.1051/m2an/2010042 Published online by Cambridge University Press

Proof. Consider the expansion of $\|\phi\|^2_{E;N}$:

$$\|\phi\|^2_{E;N} = (\phi, D_N^h \overline{\phi}^h) = \sum_{n=0}^{N} (\phi, (I - F_h)^n F_h \phi).$$

From (2.8), we have that $\|F_h\phi\| = \|\overline{\phi}^h\| \leq \|\phi\|$, and thus that $\|F_h\| \leq 1$, and $(I - F_h)$ and F_h are positive and self adjoint on V_h. Then since F_h and $(I - F_h)^n$ commute, for each term in the expansion we get

$$(\phi, (I - F_h)^n F_h \phi) = ((I - F_h)^{\frac{n}{2}} F_h^{\frac{1}{2}} \phi, (I - F_h)^{\frac{n}{2}} F_h^{\frac{1}{2}} \phi) = \|(I - F_h)^{\frac{n}{2}} F_h^{\frac{1}{2}} \phi\|^2.$$

Thus $\|\phi\|^2_{E;N}$ is a sum of nonnegative terms, the first of which is $(\phi, F_h\phi) = \|\phi\|^2_{E;0}$, and therefore we get $\|\phi\|_{E;0} \leq \|\phi\|_{E;N}$.

Also, since $\|I - F_h\| \leq 1$, we have

$$(\phi, (I - F_h)^n F_h \phi) = \|(I - F_h)^{\frac{n}{2}} F_h^{\frac{1}{2}} \phi\|^2 \leq \|F_h^{\frac{1}{2}} \phi\|^2 = (\phi, F_h\phi) = \|\phi\|^2_{E;0}.$$

Thus, $\|\phi\|^2_{E;N} \leq N\|\phi\|^2_{E;0}$, which completes the proof of the equivalence of the natural energy norms.

For the second equivalence result, consider the expansion of $\|\phi\|^2_{\epsilon;N}$:

$$\|\phi\|^2_{\epsilon;N} = -(\widetilde{\Delta}_h\phi, D_N^h \overline{\phi}^h) = \sum_{n=0}^{N} -(\widetilde{\Delta}_h\phi, (I - F_h)^n F_h \phi) = \sum_{n=0}^{N} -(F_h\widetilde{\Delta}_h\phi, (I - F_h)^n \phi). \tag{2.15}$$

Using the definition of F_h,

$$F_h\widetilde{\Delta}_h\phi = \frac{-1}{\alpha^2} F_h \left((I - \alpha^2\widetilde{\Delta}_h) - I\right)\phi = \frac{-1}{\alpha^2} F_h \left(F_h^{-1} - I\right)\phi = \frac{-1}{\alpha^2}(I - F_h)\phi. \tag{2.16}$$

Combining (2.16) and (2.15) gives

$$\|\phi\|^2_{\epsilon;N} = \sum_{n=0}^{N} \frac{1}{\alpha^2}((I - F_h)\phi, (I - F_h)^n \phi) = \sum_{n=0}^{N} \frac{1}{\alpha^2}\|(I - F_h)^{(n+1)/2}\phi\|^2.$$

Since $\frac{1}{\alpha^2}\|(I - F_h)^{\frac{1}{2}}\phi\|^2 = \|\phi\|^2_{\epsilon;0}$, using (2.4) and (2.5), we have proven that $\|\phi\|^2_{\epsilon;N}$ is a sum of positive terms, including $\|\phi\|^2_{\epsilon;0}$. Thus we have that $\|\phi\|_{\epsilon;0} \leq \|\phi\|_{\epsilon;N}$. To complete the proof, since $\|I - F_h\| \leq 1$, we note that each term in the expansion of $\|\phi\|_{\epsilon;N}$ is less than or equal to $\|\phi\|_{\epsilon;0}$. Summing these terms completes the proof. □

The following technical lemmas lead to simpler stability and convergence analysis.

Lemma 2.6. *Let $\phi \in V_h$. Then the following inequalities hold:*

$$\|D_N^h \overline{\phi}^h\| \leq N\|\phi\|_{E;0}, \qquad \|\nabla D_N^h \overline{\phi}^h\| \leq N\|\phi\|_{\epsilon;0}.$$

Proof. We prove the second (harder) inequality first. The first inequality will follow in an analogous way. This proof uses the definitions of the natural energy dissipation norms and modified discrete Laplacian, and manipulates using commutation and positive definite properties of the filter and deconvolution operator. From (2.4) we obtain

$$\|\nabla D_N^h \overline{\phi}^h\|^2 = \left(\nabla D_N^h \overline{\phi}^h, \nabla D_N^h \overline{\phi}^h\right) \leq -\left(\widetilde{\Delta}_h D_N^h \overline{\phi}^h, D_N^h \overline{\phi}^h\right).$$

https://doi.org/10.1051/m2an/2010042 Published online by Cambridge University Press

Since the filter and deconvolution operators commute and are both positive definite and self-adjoint, and also using the norm equivalence lemma, we get

$$\begin{aligned}-\left(\widetilde{\Delta}_h D_N^h \overline{\phi}^h, D_N^h \overline{\phi}^h\right) &= -\left(\widetilde{\Delta}_h D_N^{h\,\frac{1}{2}} F_h^{\frac{1}{2}}\phi, D_N^h \overline{D_N^{h\,\frac{1}{2}} F_h^{\frac{1}{2}}\phi}^h\right) = \|D_N^{h\,\frac{1}{2}} F_h^{\frac{1}{2}}\phi\|_{\epsilon;N}^2 \le N\|D_N^{h\,\frac{1}{2}} F_h^{\frac{1}{2}}\phi\|_{\epsilon;0}^2 \\ &= -N\left(\widetilde{\Delta}_h D_N^{h\,\frac{1}{2}} F_h^{\frac{1}{2}}\phi, \overline{D_N^{h\,\frac{1}{2}} F_h^{\frac{1}{2}}\phi}^h\right) = -N\left(\widetilde{\Delta}_h F_h^{\frac{1}{2}}\phi, D_N^h \overline{F_h^{\frac{1}{2}}\phi}^h\right) \\ &= N\|F_h^{\frac{1}{2}}\phi\|_{\epsilon;N}^2 \le N^2\|F_h^{\frac{1}{2}}\phi\|_{\epsilon;0}^2.\end{aligned}$$

Expanding out the last term and using the norm equivalence result as well as (2.7) yields

$$\begin{aligned}N^2\|F_h^{\frac{1}{2}}\phi\|_{\epsilon;0}^2 = -N^2(\widetilde{\Delta}_h\overline{\phi}^h, \overline{\phi}^h) &= N^2\left(\|\nabla\overline{\phi}^h\|^2 + \frac{\gamma}{\nu}\|\nabla\cdot\overline{\phi}^h\|^2\right) \\ &\le N^2\left((\nabla\phi, \nabla\overline{\phi}^h) + \frac{\gamma}{\nu}(\nabla\cdot\phi, \nabla\cdot\overline{\phi}^h)\right) = N^2\|\phi\|_{\epsilon;0}^2,\end{aligned}$$

which completes the proof. □

Lemma 2.7. *For $\phi \in V_h$, the following inequalities hold:*

$$\gamma\|\nabla\cdot\overline{\phi}^h\|^2 \le \nu\|\phi\|_{\epsilon;0}^2, \tag{2.17}$$

$$\|\overline{\phi}^h\|_{\epsilon;0} \le \|\phi\|_{\epsilon;0}, \tag{2.18}$$

$$\gamma\|\nabla\cdot D_N^h\overline{\phi}^h\|^2 \le C(N)\nu\|\phi\|_{\epsilon;N}^2. \tag{2.19}$$

Proof. The first inequality is a direct consequence of (2.7). For the second inequality, expanding the difference of squares of the terms gives

$$\|\phi\|_{\epsilon;0}^2 - \|\overline{\phi}^h\|_{\epsilon;0}^2 = (\nabla\phi, \nabla\overline{\phi}^h) + \frac{\gamma}{\nu}(\nabla\cdot\phi, \nabla\cdot\overline{\phi}^h) - \left(\nabla\overline{\phi}^h, \nabla\overline{\overline{\phi}^h}^h\right) - \frac{\gamma}{\nu}\left(\nabla\cdot\overline{\phi}^h, \nabla\cdot\overline{\overline{\phi}^h}^h\right).$$

Equations (2.7) and (2.10) now imply the difference is positive. For the last inequality, expand the deconvolution operator as a sum with coefficients β_n, and use (2.17), as

$$\gamma\|\nabla\cdot D_N^h\overline{\phi}^h\|^2 \le \sum_{n=0}^{N}\beta_n\gamma\|\nabla\cdot F_h^n\overline{\phi}^h\|^2 \le \sum_{n=0}^{N}\beta_n\gamma\|\nabla\cdot\overline{F_h^n\phi}^h\|^2 \le \sum_{n=0}^{N}\beta_n\nu\|F_h^n\phi\|_{\epsilon;0}^2.$$

Applying (2.18) now gives

$$\sum_{n=0}^{N}\beta_n\nu\|F_h^n\phi\|_{\epsilon;0}^2 \le \sum_{n=0}^{N}\beta_n\nu\|\phi\|_{\epsilon;0}^2 \le C(N)\nu\|\phi\|_{\epsilon;0}^2 \le C(N)\nu\|\phi\|_{\epsilon;N}^2.$$ □

The lemmas below provide necessary estimates involving the new grad-div modified Laplacian and the van Cittert operator D_N^h. Due to the similarity of the proofs with those in [32], we omit them herein.

Lemma 2.8. *The operators $D_N : L^2(\Omega) \to L^2(\Omega)$ and $D_N^h : V_h \to V_h$ are bounded, self-adjoint positive operators. For $\phi \in L^2(\Omega)$,*

$$\phi = D_N\overline{\phi} + (-1)^{(N+1)}\alpha^{2N+2}\Delta^{N+1}F^{N+1}\phi,$$

https://doi.org/10.1051/m2an/2010042 Published online by Cambridge University Press

and for $\phi \in V_h$,

$$\phi = D_N^h \overline{\phi}^h + (-1)^{(N+1)} \alpha^{2N+2} \widetilde{\Delta}_h^{N+1} F_h^{N+1} \phi.$$

Proof. The proof is based on an algebraic identity, following [5]. □

The following lemma is the key to reducing the error arising from the consistency of the model.

Lemma 2.9. *For divergence free* $\phi \in H_0^{2N+2}$ *(or* $\phi \in H^{2N+2}$ *is zero mean periodic), the discrete approximate deconvolution operator defined on the inf-sup stable spaces of continuous piecewise polynomial* (P_k, P_{k-1}) *satisfies*

$$\begin{aligned} \|\phi - D_N^h \overline{\phi}^h\| \quad &\leq \quad C(N) h^k \left(\frac{\nu^{1/2}}{\alpha \gamma^{1/2}} + \alpha + h + \frac{\alpha \gamma^{1/2}}{\nu^{1/2}} \right) \left(\sum_{n=0}^{N} | \ F^n \overline{\phi} \ |_{k+1} \right) \\ &\quad + C \alpha^{2N+2} \|\Delta^{N+1} F^{N+1} \phi\|. \end{aligned} \tag{2.20}$$

Remark 2.10. When ϕ lacks the smoothness required for Lemma 2.9, the error caused by applying discrete deconvolution is of the same order as the filtering error. If ϕ is divergence free but only satisfies $\phi \in X$ and $\Delta \phi \in L^2(\Omega)$, then it can be shown that

$$\begin{aligned} ||\phi - D_N^h \overline{\phi}^h|| \leq C(N) \inf_{v^h \in V^h} (||\phi - v^h||^2 + \alpha^2 ||\nabla(\phi - v^h)||^2 + \frac{\alpha^2 \gamma}{\nu} ||\nabla \cdot (\phi - v^h)||^2)^{\frac{1}{2}} \\ + C(N) \left(\alpha^2 ||\Delta \phi|| + \alpha \sqrt{\frac{\gamma}{\nu}} \|\nabla \cdot \phi\| \right). \end{aligned}$$

Proof. We start the proof by splitting the error

$$\|\phi - D_N^h \overline{\phi}^h\| \leq \|\phi - D_N \overline{\phi}\| + \|D_N \overline{\phi} - D_N^h \overline{\phi}\| + \|D_N^h \overline{\phi} - D_N^h \overline{\phi}^h\|. \tag{2.21}$$

For the first term, Lemma 2.8 gives

$$\|\phi - D_N \overline{\phi}\| \leq C \, \alpha^{2N+2} \|\Delta^{N+1} F^{N+1} \phi\|. \tag{2.22}$$

Analysis of the second and third terms relies on an estimate for $\|\overline{\phi} - \overline{\phi}^h\|$, and so we derive this first. From the definitions of the discrete and continuous filters, we have for $v_h \in V_h$,

$$\begin{aligned} (\overline{\phi}, v_h) + \alpha^2 (\nabla \overline{\phi}, \nabla v_h) + \frac{\alpha^2 \gamma}{\nu} (\nabla \cdot \overline{\phi}, \nabla \cdot v_h) - (\lambda, \nabla \cdot v_h) \quad &= \quad (\phi, v_h), \\ (\overline{\phi}^h, v_h) + \alpha^2 (\nabla \overline{\phi}^h, \nabla v_h) + \frac{\alpha^2 \gamma}{\nu} (\nabla \cdot \overline{\phi}^h, \nabla \cdot v_h) \quad &= \quad (\phi, v_h). \end{aligned}$$

Subtracting these equations, defining $e := \overline{\phi} - \overline{\phi}^h$, decomposing e into its parts in and out of V_h by $e = (\overline{\phi} - \Phi) + (\Phi - \overline{\phi}^h) =: s + r_h$, where Φ is the L^2 projection of $\overline{\phi}$ into V_h, gives for every $v_h \in V_h$,

$$(r_h, v_h) + \alpha^2 (\nabla r_h, \nabla v_h) + \frac{\alpha^2 \gamma}{\nu} (\nabla \cdot r_h, \nabla \cdot v_h) = (\lambda, \nabla \cdot v_h) + (s, v_h) + \alpha^2 (\nabla s, \nabla v_h) + \frac{\alpha^2 \gamma}{\nu} (\nabla \cdot s, \nabla \cdot v_h). \tag{2.23}$$

Since $v_h \in V_h$, $(\lambda, \nabla \cdot v_h) = (\lambda - q_h, \nabla \cdot v_h)$. Using this, choosing $v_h = r_h$, and applying Cauchy-Schwarz and Young's inequalities yields

$$\|r_h\|^2 + \alpha^2 \|\nabla r_h\|^2 + \frac{\alpha^2 \gamma}{\nu} \|\nabla \cdot r_h\|^2 \leq \inf_{q_h \in Q_h} \|\lambda - q_h\| \|\nabla \cdot r_h\| + \|s\|^2 + \alpha^2 \|\nabla s\|^2 + \frac{\alpha^2 \gamma}{\nu} \|\nabla \cdot s\|^2. \tag{2.24}$$

https://doi.org/10.1051/m2an/2010042 Published online by Cambridge University Press

We bound the pressure term using Young's inequality as

$$\inf_{q_h \in Q_h} \|\lambda - q_h\| \|\nabla \cdot r_h\| \leq \frac{\nu}{2\alpha^2\gamma} \inf_{q_h \in Q_h} \|\lambda - q_h\|^2 + \frac{\alpha^2\gamma}{2\nu} \|\nabla \cdot r_h\|^2. \tag{2.25}$$

Inserting the bound (2.25) into (2.24), using the triangle inequality and dropping positive terms on the left hand side, then taking square roots implies

$$\|\overline{\phi} - \overline{\phi}^h\| \leq C \left(\frac{\nu^{1/2}}{\alpha\gamma^{1/2}} h^{s+1} |\lambda|_{s+1} + h^{k+1} |\overline{\phi}|_{k+1} + h^k \alpha |\overline{\phi}|_{k+1} + h^k \frac{\alpha\gamma^{1/2}}{\nu^{1/2}} |\overline{\phi}|_{k+1} \right). \tag{2.26}$$

Since from the filter equation we have that $|\lambda|_k \leq |\overline{\phi}|_{k+1}$, and with the assumption of (P_k, P_{k-1}) elements, (2.26) becomes

$$\|\overline{\phi} - \overline{\phi}^h\| \leq C h^k |\overline{\phi}|_{k+1} \left(\frac{\nu^{\frac{1}{2}}}{\alpha\gamma^{\frac{1}{2}}} + h + \alpha + \frac{\alpha\gamma^{1/2}}{\nu^{1/2}} \right).$$

For the third term in (2.21), we use the fact that D_N^h is a polynomial in the bounded operator F_h, and so

$$\begin{aligned} \|D_N^h \overline{\phi} - D_N^h \overline{\phi}^h\| &\leq C(N+1) \|\overline{\phi} - \overline{\phi}^h\| \\ &\leq C(N+1) h^k |\overline{\phi}|_{k+1} \left(\frac{\nu^{\frac{1}{2}}}{\alpha\gamma^{\frac{1}{2}}} + h + \alpha + \frac{\alpha\gamma^{1/2}}{\nu^{1/2}} \right). \end{aligned}$$

It is left to bound the second term from (2.21); we do so for the general Nth case. From the definitions of D_N and D_N^h, it is clear that both $D_N^h \overline{\phi}$ and $D_N^h \overline{\phi}$ can be written as polynomials in their respective filters, with matching coefficients. Note that since N is typically chosen less than 5 or 6, the coefficients are $O(1)$. Thus we have that

$$\|D_N \overline{\phi} - D_N^h \overline{\phi}\| = \left\| \sum_{n=0}^{N} \beta_n \left(F^n \overline{\phi} - (F_h)^n \overline{\phi} \right) \right\| \leq \sum_{n=0}^{N} \beta_n \|F^n \overline{\phi} - (F_h)^n \overline{\phi}\|,$$

and we will consider this sum starting at $n = 1$, the first non zero term. Thus we now desire a bound on the difference in the filters applied multiple times, so we add and subtract terms with mixed continuous and discrete filtering. Hence,

$$\begin{aligned} \sum_{n=1}^{N} \beta_n \|F^n \overline{\phi} - (F_h)^n \overline{\phi}\| = \sum_{n=1}^{N} \beta_n \|(F^n \overline{\phi} - F_h F^{n-1} \overline{\phi}) \\ + (F_h F^{n-1} \overline{\phi} - F_h^2 F^{n-2} \overline{\phi}) + \ldots + (F_h^{n-1} F \overline{\phi} - F_h^n \overline{\phi})\|. \end{aligned} \tag{2.27}$$

Applying the triangle inequality to (2.27) yields

$$\begin{aligned} \sum_{n=1}^{N} \beta_n \|F^n \overline{\phi} - (F_h)^n \overline{\phi}\| \leq \sum_{n=1}^{N} \beta_n (\|F^n \overline{\phi} - F_h F^{n-1} \overline{\phi}\| \\ + \|F_h F^{n-1} \overline{\phi} - F_h^2 F^{n-2} \overline{\phi}\| + \ldots + \|F_h^{n-1} F \overline{\phi} - F_h^n \overline{\phi}\|). \end{aligned} \tag{2.28}$$

https://doi.org/10.1051/m2an/2010042 Published online by Cambridge University Press

Using the bound $\|F_h\| \leq 1$, and factoring $F^{n-i}\overline{\phi}$ in each norm, (2.28) can be further reduced to

$$\sum_{n=1}^{N} \beta_n \|F^n\overline{\phi} - (F_h)^n\overline{\phi}\| \leq \sum_{n=1}^{N} \beta_n (\|(F-F_h)(F^{n-1}\overline{\phi})\| + \|(F-F_h)(F^{n-2}\overline{\phi})\| + ... + \|(F-F_h)(F^0\overline{\phi})\|)$$
$$\leq \sum_{n=1}^{N} Ch^k \left(\frac{\nu^{1/2}}{\alpha\gamma^{1/2}} + h + \alpha + \frac{\alpha\gamma^{1/2}}{\nu^{1/2}}\right) (|F^n\overline{\phi}|_{k+1} + |F^{n-1}\overline{\phi}|_{k+1} + ... + |\overline{\phi}|_{k+1}),$$

and now substituting into (2.21) finishes the proof. □

Remark 2.11. There remains the question of uniform in α bound of the last term, $|F^n\phi|_{k+1}$, in (2.20). This is a question about uniform-regularity of an elliptic-elliptic singular perturbation problem and some results are proven in [30]. To summarize, in the periodic case it is very easy to show by Fourier series that for all k

$$|F^n\phi|_{k+1} \leq C|\phi|_{k+1}. \tag{2.29}$$

The non-periodic case can be more delicate. Suppose $\partial\Omega \in C^{k+3}$ and $\phi = 0$ on $\partial\Omega$ (*i.e.* $\phi \in H_0^1(\Omega) \bigcap H^{k+1}(\Omega)$). Then it is known that $\overline{\phi} \in H^{k+3}(\Omega) \bigcap H_0^1(\Omega)$, and $\Delta\overline{\phi} = 0$ on $\partial\Omega$. Further,

$$\|\overline{\phi}\|_j \leq C\|\phi\|_j \qquad j = 0, 1, 2.$$

So, (2.29) holds for $k = -1, 0, +1$. It also holds for higher values of k provided additionally $\Delta^j\phi = 0$ on $\partial\Omega$ for $0 \leq j \leq \left[\frac{k+1}{2}\right] - 1$.

Now consider the second term $n = 2$ *i.e.* $F^2\phi = \overline{\overline{\phi}}$. We know from elliptic theory for $\phi \in H^{k+1}(\Omega) \bigcap H_0^1(\Omega)$, that $\overline{\phi} \in H^{k+3}(\Omega) \bigcap H_0^1(\Omega)$, (as noted above) $\Delta\overline{\phi} = 0$ on $\partial\Omega$ and

$$-\delta^2\Delta\overline{\overline{\phi}} + \overline{\overline{\phi}} = \overline{\phi} \text{ in } \Omega, \text{ and } \overline{\phi} = \Delta\overline{\phi} = 0 \text{ on } \partial\Omega.$$

Theorem 1.1 in [30] then implies, uniformly in α,

$$\|\overline{\overline{\phi}}\|_j \leq C\|\overline{\phi}\|_j, \quad j = 0, 1, 2, 3, 4.$$

This extends directly to $F^n\phi$.

The next results and definitions will be important in the convergence analysis, see Section 4.

Lemma 2.12. *Assume $u \in C^0(t^n, t^{n+1}; L^2(\Omega))$. If u is twice differentiable in time and $u_{tt} \in L^2((t^n, t^{n+1}) \times \Omega)$ then*

$$\|u^{n+\frac{1}{2}} - u(t^{n+\frac{1}{2}})\|^2 \leq \frac{1}{48}(\Delta t)^3 \int_{t^n}^{t^{n+1}} \|u_{tt}\|^2 \, \mathrm{d}t.$$

If $u_t \in C^0(t^n, t^{n+1}; L^2(\Omega))$ and $u_{ttt} \in L^2((t^n, t^{n+1}) \times \Omega)$ then

$$\left\| \frac{u^{n+1} - u^n}{\Delta t} - u_t(t^{n+\frac{1}{2}}) \right\|^2 \leq \frac{1}{1280}(\Delta t)^3 \int_{t^n}^{t^{n+1}} \|u_{ttt}\|^2 \, \mathrm{d}t.$$

If $\nabla u \in C^0(t^n, t^{n+1}; L^2(\Omega))$ and $\nabla u_{tt} \in L^2((t^n, t^{n+1}) \times \Omega)$ then

$$\|\nabla(u^{n+\frac{1}{2}} - u(t^{n+\frac{1}{2}}))\|^2 \leq \frac{(\Delta t)^3}{48} \int_{t^n}^{t^{n+1}} \|\nabla u_{tt}\|^2 \, \mathrm{d}t.$$

https://doi.org/10.1051/m2an/2010042 Published online by Cambridge University Press

In the discrete case we use the analogous norms:

$$|||v|||_{\infty,k} := \max_{0\le n\le M} \|v^n\|_k, \qquad |||v_{\frac12}|||_{\infty,k} := \max_{1\le n\le M} \|v^{n-\frac12}\|_k,$$

$$|||v|||_{m,k} := \left(\sum_{n=0}^{M} \|v^n\|_k^m \Delta t\right)^{1/m}, \qquad |||v_{\frac12}|||_{m,k} := \left(\sum_{n=1}^{M} \|v^{n-\frac12}\|_k^m \Delta t\right)^{1/m}.$$

Further in analysis we use the following properties of the nonlinear term.

Lemma 2.13. *For $u, v, w \in X$ and $\nabla \times v \in L^\infty(\Omega)$,*

$$\begin{aligned}
|\,(u\times\nabla\times v, w)\,| &\le C\,\|u\|\|\nabla\times v\|_\infty\|w\|,\\
|\,(u\times\nabla\times v, w)\,| &\le C\,\|\nabla u\|\|\nabla\times v\|\|\nabla w\|,\\
|\,(u\times\nabla\times v, w)\,| &\le C\,\|u\|^{\frac12}\|\nabla u\|^{\frac12}\|\nabla\times v\|\|\nabla w\|,\\
|\,(u\times\nabla\times v, w)\,| &\le C\,\|\nabla u\|\|\nabla\times v\|\|w\|^{\frac12}\|\nabla w\|^{\frac12}.
\end{aligned}$$

3. A time-stepping scheme for NS-α and its stability

To discretize (2.2) in time we apply the Crank-Nicolson type scheme. We assume that initial velocity u_h^0, forcing term f, a filtering radius $\alpha > 0$, kinematic viscosity $\nu > 0$, stabilization parameter $\gamma \ge 0$, approximate deconvolution order $N \ge 0$, timestep $\Delta t > 0$, and the endtime $T \ge \Delta t$ are given. Let $v(t^{n+\frac12}) = v((t^{n+1}+t^n)/2)$ for the continuous variables, and $v^{n+\frac12} = (v^{n+1}+v^n)/2$ for both the continuous and discrete variables. With the notation given in the previous section one may write down the scheme in the compact form of Algorithm 3.1 below.

Algorithm 3.1. *Set $M = \frac{T}{\Delta t}$ and for $n = 0, 2, ..., M-1$, find $u_h^n \in V_h$ satisfying $\forall v_h \in V_h$,*

$$\frac{1}{\Delta t}(u_h^{n+1} - u_h^n, v_h) - \left(D_N^h \overline{u_h^{n+\frac12}}^h \times \nabla \times u_h^{n+\frac12}, v_h\right) - \nu(\widetilde{\Delta}_h u_h^{n+\frac12}, v_h) = \left(f(t^{n+\frac12}), v_h\right). \tag{3.1}$$

Remark 3.2. In some situations, it may be advantageous to linearize the scheme *via* the method of Baker [3], using $D_N^h \overline{u_h^{n+\frac12}}^h \times \nabla \times u_h^*$ in the second term of (3.1) with $u_h^* = \frac32 u_h^n - \frac12 u_h^{n-1}$. This linear problem will have identical stability and convergence results as that of the nonlinear scheme (3.1).

Lemma 3.3. *Algorithm 3.1 is unconditionally stable. Its solutions satisfy*

$$\|u_h^M\|_{E;N}^2 + \nu\Delta t \sum_{n=0}^{M-1} \|u_h^{n+\frac12}\|_{\epsilon;N}^2 \le \|u_h^0\|_{E;N}^2 + \frac{N^2}{\nu}\Delta t \sum_{n=0}^{M-1} \|f(t^{n+\frac12})\|_{H^{-1}}^2.$$

Proof. Choose $v_h = D_N^h \overline{u_h^{n+\frac12}}^h$ in (3.1). The nonlinear term vanishes, and switching to the natural energy and energy dissipation norms yields

$$\frac{1}{2\Delta t}\left(\|u_h^{n+1}\|_{E;N}^2 - \|u_h^n\|_{E;N}^2\right) + \nu\|u_h^{n+\frac12}\|_{\epsilon;N}^2 = \left(f(t^{n+\frac12}), D_N^h \overline{u_h^{n+\frac12}}^h\right). \tag{3.2}$$

https://doi.org/10.1051/m2an/2010042 Published online by Cambridge University Press

We majorize the right hand side term first by using using Cauchy-Schwarz, Young's inequality and Lemma 2.6 with (2.14) to get

$$\left(f(t^{n+\frac{1}{2}}), D_N^h \overline{u_h^{n+\frac{1}{2}}}^h\right) \le \|f(t^{n+\frac{1}{2}})\|_{H^{-1}} \left\|\nabla D_N^h \overline{u_h^{n+\frac{1}{2}}}^h\right\| \le N\|f(t^{n+\frac{1}{2}})\|_{H^{-1}} \|u_h^{n+\frac{1}{2}}\|_{\epsilon;N}$$
$$\le \frac{N^2}{2\nu}\|f(t^{n+\frac{1}{2}})\|_{H^{-1}}^2 + \frac{\nu}{2}\|u_h^{n+\frac{1}{2}}\|_{\epsilon;N}^2. \tag{3.3}$$

Combining (3.2) and (3.3), and multiplying both sides by $2\Delta t$ gives

$$\left(\|u_h^{n+1}\|_{E;N}^2 - \|u_h^n\|_{E;N}^2\right) + \nu\Delta t\|u_h^{n+\frac{1}{2}}\|_{\epsilon;N}^2 \le \frac{N^2\Delta t}{\nu}\|f(t^{n+\frac{1}{2}})\|_{H^{-1}}^2.$$

Summing from $n = 0$ to $M-1$ provides the estimate

$$\|u_h^M\|_{E;N}^2 + \nu\Delta t\sum_{n=0}^{M-1}\|u_h^{n+\frac{1}{2}}\|_{\epsilon;N}^2 \le \|u_h^0\|_{E;N}^2 + \frac{N^2}{\nu}\Delta t\sum_{n=0}^{M-1}\|f(t^{n+\frac{1}{2}})\|_{H^{-1}}^2. \qquad \square$$

4. Analysis of full Crank-Nicolson scheme

In this section, we show that solutions of the scheme (3.1), are unconditionally stable, well defined and optimally convergent to solutions of the NSE. Our main convergence estimates are given next.

Theorem 4.1. *Let $(u(t), p(t))$ be a smooth strong solution of the NSE (see,* e.g. [31]*) such that the norms of $(u(t), p(t))$ on the right hand side of (4.1)–(4.3) are finite. Assume (2.1) with some $k \ge 1$, $s \ge 0$ and suppose (u_h^0, q_h^0) are approximations of $(u(0), p(0))$ to the accuracy of (2.1), respectively. Then for $\triangle t$ small enough, $\alpha = O(h)$, and γ chosen to satisfy $\frac{\nu}{\alpha^2\gamma} \le O(1)$, there is a constant $C = C(u,p)$ such that*

$$|||u - u_h|||_{\infty,0} \le F(\Delta t, h, \alpha) + Ch^{k+1}|||u|||_{\infty,k+1}, \tag{4.1}$$

$$\left(\nu\Delta t\sum_{n=0}^{M-1}\|\nabla(u^{n+\frac{1}{2}} - u_h^{n+\frac{1}{2}})\|^2\right)^{\frac{1}{2}} \le F(\Delta t, h, \alpha) + C\nu^{\frac{1}{2}}h^k|||u|||_{2,k+1}, \tag{4.2}$$

where

$$F(\Delta t, h, \alpha) := C^*\Big\{CN(\nu^{\frac{1}{2}} + \gamma^{\frac{1}{2}})h^k|||u|||_{2,k+1} + CN^2\nu^{-\frac{1}{2}}h^k\left(|||u|||_{4,k+1}^2 + |||\nabla u|||_{2,0}^2\right)$$
$$+ CN\gamma^{-\frac{1}{2}}h^{s+1}|||p_{\frac{1}{2}}|||_{2,s+1} + CN\nu^{-\frac{1}{2}}\alpha^{2N+2}|||\Delta^{N+1}F^{N+1}u_{\frac{1}{2}}|||_{2,0}$$
$$+ CN\nu^{-\frac{1}{2}}h^k(\alpha^{-1}\gamma^{-\frac{1}{2}}\nu^{\frac{1}{2}} + \alpha + h + \alpha\gamma^{\frac{1}{2}}\nu^{-\frac{1}{2}})\left(\sum_{l=0}^{N}|||\ F^l\,\overline{u}_{\frac{1}{2}}\ |||_{2,k+1}\right)$$
$$+ CN(\Delta t)^2\Big(\|u_{ttt}\|_{2,0} + \gamma^{-\frac{1}{2}}\|p_{tt}\|_{2,0} + \|f_{tt}\|_{2,0} + (\nu^{\frac{1}{2}} + \gamma^{\frac{1}{2}})\|\nabla u_{tt}\|_{2,0}$$
$$+ \nu^{-\frac{1}{2}}\|\nabla u_{tt}\|_{4,0}^2 + \nu^{-\frac{1}{2}}|||\nabla u|||_{4,0}^2 + \nu^{-\frac{1}{2}}|||\nabla u_{\frac{1}{2}}|||_{4,0}^2\Big)\Big\}. \tag{4.3}$$

Remark 4.2. The theorem shows that the addition of grad-div stabilization does affect (improve) convergence of the new scheme. The velocity error is not scaled as *Re* * pressure error, as would be the case without stabilization. If $\gamma = 0$, the treatment of the pressure term in the convergence proof would need handled in the usual way, which leads to the undesirable scaling: with $\nu^{-\frac{1}{2}}$ in all instances where $\gamma^{-\frac{1}{2}}$ appears in (4.3).

https://doi.org/10.1051/m2an/2010042 Published online by Cambridge University Press

On the other hand, the error due to the filtered velocity is scaled by $\alpha\gamma^{\frac{1}{2}}\nu^{-1}$. This scaling comes from the grad-div stabilization of the filter, and suggests that for very small ν the parameter γ in the filter might need to be reduced accordingly. Our analysis does not cover, however, the case of different stabilization parameters in momentum and filter equations. As shown in [16] using no stabilization in filtering still leads to a reasonable numerical results, although theoretical analysis becomes rather limited and for comparison the results found herein for the 2D step problem are superior to those of [16].

Corollary 4.3. *Suppose that in addition to the assumptions made in Theorem 4.1, the finite element spaces X^h and Q^h are composed of (P_k, P_{k-1}) polynomial elements with order $k \geq 1$. Suppose that the indicated norms on the right hand side of (4.1)–(4.3) are finite. Then the error in the Crank-Nicolson finite element scheme for NS-α with approximate deconvolution is of the order*

$$\|\|u - u_h\|\|_{\infty,0} + \left(\nu\Delta t \sum_{n=1}^{M} \|\nabla(u^{n+\frac{1}{2}} - u_h^{n+\frac{1}{2}})\|^2\right)^{\frac{1}{2}} = O(h^k + \Delta t^2 + h^{2N+2}). \tag{4.4}$$

Remark 4.4. The restriction of γ to satisfy $\nu < O(\gamma\alpha^2)$ is very weak since it is only when ν is small that a model would be used.

Proof of Theorem 4.1. At time $t^{n+\frac{1}{2}}$, u from the NSE solution satisfies

$$\begin{aligned}\left(\frac{u^{n+1}-u^n}{\Delta t}, v_h\right) + \nu(\nabla u^{n+\frac{1}{2}}, \nabla v_h) + \gamma(\nabla\cdot u^{n+\frac{1}{2}}, \nabla\cdot v_h)\\ -\left(D_N^h \overline{u^{n+\frac{1}{2}}}^h \times \nabla\times u^{n+\frac{1}{2}}, v_h\right) - (p^{n+\frac{1}{2}}, \nabla\cdot v_h)\\ = (f^{n+\frac{1}{2}}, v^h) + Intp(u^n, p^n; v_h),\end{aligned} \tag{4.5}$$

for all $v_h \in V_h$, where $Intp(u^n, p^n; v_h)$, representing the interpolating error, denotes

$$\begin{aligned}Intp(u^n, p^n; v_h) = &\left(\frac{u^{n+1}-u^n}{\Delta t} - u_t(t^{n+\frac{1}{2}}), v_h\right) + \nu(\nabla u^{n+\frac{1}{2}} - \nabla u(t^{n+\frac{1}{2}}), \nabla v_h)\\ &+ \gamma(\nabla\cdot u^{n+\frac{1}{2}} - \nabla\cdot u(t^{n+\frac{1}{2}}), \nabla\cdot v_h)\\ &- \left(D_N^h \overline{u^{n+\frac{1}{2}}}^h \times \nabla\times u^{n+\frac{1}{2}}, v_h\right) - \left(u(t^{n+\frac{1}{2}}) \times \nabla\times u(t^{n+\frac{1}{2}}), v_h\right)\\ &- \left(p^{n+\frac{1}{2}} - p(t^{n+\frac{1}{2}}), \nabla\cdot v_h\right) + \left(f(t^{n+\frac{1}{2}}) - f^{n+\frac{1}{2}}, v_h\right),\end{aligned} \tag{4.6}$$

since $(\nabla\cdot u, q) = 0\ \forall q \in Q$.

Subtracting (4.5) from (3.1) and letting $e^n = u^n - u_h^n$, we have

$$\begin{aligned}\frac{1}{\Delta t}(e^{n+1} - e^n, v_h) + \nu(\nabla e^{n+\frac{1}{2}}, \nabla v_h) + \gamma(\nabla\cdot e^{n+\frac{1}{2}}, \nabla\cdot v_h)\\ = \left(D_N^h \overline{u^{n+\frac{1}{2}}}^h \times \nabla\times u^{n+\frac{1}{2}}, v_h\right) - \left(D_N^h \overline{u_h^{n+\frac{1}{2}}}^h \times \nabla\times u_h^{n+\frac{1}{2}}, v_h\right)\\ + (p^{n+\frac{1}{2}}, \nabla\cdot v_h) + Intp(u^n, p^n; v_h), \quad \forall v_h \in V_h.\end{aligned} \tag{4.7}$$

Decompose the error as $e^n = (u^n - U^n) - (u_h^n - U^n) := \eta^n - \phi_h^n$ where $\phi_h^n \in V_h$, and U is the L^2 projection of u in V_h. Setting $v_h = D_N^h \overline{\phi_h^{n+\frac{1}{2}}}^h$ in (4.7), using $\left(q, \nabla\cdot D_N^h \overline{\phi_h^{n+\frac{1}{2}}}^h\right) = 0$ for all $q \in Q_h$, equations (2.4) and (2.12),

https://doi.org/10.1051/m2an/2010042 Published online by Cambridge University Press

we obtain

$$\begin{aligned}\left(\phi_h^{n+1}-\phi_h^n, D_N^h\overline{\phi_h^{n+\frac12}}^h\right)+\nu\Delta t\|\phi_h^{n+\frac12}\|_{\epsilon,N}^2 &= \left(\eta^{n+1}-\eta^n, D_N^h\overline{\phi_h^{n+\frac12}}^h\right)\\ &+\nu\Delta t\left(\nabla\eta^{n+\frac12},\nabla D_N^h\overline{\phi_h^{n+\frac12}}^h\right)-\gamma\Delta t\left(\nabla\cdot\eta^{n+\frac12},\nabla\cdot D_N^h\overline{\phi_h^{n+\frac12}}^h\right)\\ &-\Delta t\left(D_N^h\overline{u_h^{n+\frac12}}^h\times\nabla\times u_h^{n+\frac12}, D_N^h\overline{\phi_h^{n+\frac12}}^h\right)-\Delta t\left(D_N^h\overline{u^{n+\frac12}}^h\times\nabla\times u^{n+\frac12}, D_N^h\overline{\phi_h^{n+\frac12}}^h\right)\\ &+\Delta t\left(p^{n+\frac12}-q,\nabla\cdot D_N^h\overline{\phi_h^{n+\frac12}}^h\right)+\Delta t\,Intp\left(u^n,p^n;D_N^h\overline{\phi_h^{n+\frac12}}^h\right),\end{aligned}\tag{4.8}$$

or rewriting the nonlinear terms,

$$\begin{aligned}\frac12(\|\phi_h^{n+1}\|_{E,N}^2-\|\phi_h^n\|_{E,N}^2)+\nu\Delta t\|\phi_h^{n+\frac12}\|_{\epsilon,N}^2 &\\ =\left(\eta^{n+1}-\eta^n, D_N^h\overline{\phi_h^{n+\frac12}}^h\right)-\nu\Delta t\left(\nabla\eta^{n+\frac12},\nabla D_N^h\overline{\phi_h^{n+\frac12}}^h\right)&\\ -\gamma\Delta t\left(\nabla\cdot\eta^{n+\frac12},\nabla\cdot D_N^h\overline{\phi_h^{n+\frac12}}^h\right)+\Delta t\left(D_N^h\overline{u^{n+\frac12}}^h\times\nabla\times\eta^{n+\frac12}, D_N^h\overline{\phi_h^{n+\frac12}}^h\right)&\\ -\Delta t\left(D_N^h\overline{u^{n+\frac12}}^h\times\nabla\times\phi_h^{n+\frac12}, D_N^h\overline{\phi_h^{n+\frac12}}^h\right)+\Delta t\left(D_N^h\overline{\eta^{n+\frac12}}^h\times\nabla\times\eta^{n+\frac12}, D_N^h\overline{\phi_h^{n+\frac12}}^h\right)&\\ -\Delta t\left(D_N^h\overline{\eta^{n+\frac12}}^h\times\nabla\times\phi_h^{n+\frac12}, D_N^h\overline{\phi_h^{n+\frac12}}^h\right)-\Delta t\left(D_N^h\overline{\eta^{n+\frac12}}^h\times\nabla\times u^{n+\frac12}, D_N^h\overline{\phi_h^{n+\frac12}}^h\right)&\\ +\Delta t\left(p^{n+\frac12}-q,\nabla\cdot D_N^h\overline{\phi_h^{n+\frac12}}^h\right)+\Delta t\,Intp\left(u^n,p^n;D_N^h\overline{\phi_h^{n+\frac12}}^h\right),&\end{aligned}\tag{4.9}$$

since $\left(D_N^h\overline{\phi_h^{n+\frac12}}^h\times\nabla\times u^{n+\frac12}, D_N^h\overline{\phi_h^{n+\frac12}}^h\right)=0.$

We now bound the terms in the RHS of (4.9) individually, using that, according to the choice of U, it holds $\left(\eta^{n+1}-\eta^n, D_N^h\overline{\phi_h^{n+\frac12}}^h\right)=0.$

Cauchy-Schwarz and Young's inequalities, together with Lemma 2.6 for the first term and Lemma 2.7 for the last two terms, give

$$\begin{aligned}\nu\Delta t\left(\nabla\eta^{n+\frac12},\nabla D_N^h\overline{\phi_h^{n+\frac12}}^h\right)&\le\nu\Delta t\|\nabla\eta^{n+\frac12}\|\left\|\nabla D_N^h\overline{\phi_h^{n+\frac12}}^h\right\|\\ &\le\frac{\nu\Delta t}{16}\|\phi_h^{n+\frac12}\|_{\epsilon,N}^2+C\nu N^2\Delta t\|\nabla\eta^{n+\frac12}\|^2,\end{aligned}\tag{4.10}$$

https://doi.org/10.1051/m2an/2010042 Published online by Cambridge University Press

$$\gamma\Delta t\left(\nabla\cdot\eta^{n+\frac12},\nabla\cdot D_N^h\overline{\phi_h^{n+\frac12}}^h\right)\le C\gamma\Delta t\|\nabla\cdot\eta^{n+\frac12}\|\left\|\nabla\cdot D_N^h\overline{\phi_h^{n+\frac12}}^h\right\|$$
$$\le\frac{\nu\Delta t}{16}\|\phi_h^{n+\frac12}\|_{\epsilon,N}^2+C(N)\gamma\Delta t\|\nabla\eta^{n+\frac12}\|^2, \tag{4.11}$$

$$\Delta t\left(p^{n+\frac12}-q,\nabla\cdot D_N^h\overline{\phi_h^{n+\frac12}}^h\right)\le\Delta t\|p^{n+\frac12}-q\|\left\|\nabla\cdot D_N^h\overline{\phi_h^{n+\frac12}}^h\right\|$$
$$\le C(N)\Delta t\sqrt{\frac{\nu}{\gamma}}\,\|\phi_h^{n+\frac12}\|_{\epsilon,N}\|p^{n+\frac12}-q\|$$
$$\le\frac{\nu\Delta t}{16}\|\phi_h^{n+\frac12}\|_{\epsilon,N}^2+C(N)\Delta t\gamma^{-1}\|p^{n+\frac12}-q\|^2. \tag{4.12}$$

Lemmas 2.13, 2.5, 2.6, equivalence of norms (Rem. 2.4) and standard inequalities give

$$\Delta t\left(D_N^h\overline{u^{n+\frac12}}^h\times\nabla\times\eta^{n+\frac12},D_N^h\overline{\phi_h^{n+\frac12}}^h\right)\le C\Delta t\left\|\nabla D_N^h\overline{u^{n+\frac12}}^h\right\|\|\nabla\eta^{n+\frac12}\|\left\|\nabla D_N^h\overline{\phi_h^{n+\frac12}}^h\right\|$$
$$\le\frac{\nu\Delta t}{16}\|\phi_h^{n+\frac12}\|_{\epsilon,N}^2+CN^4\,\nu^{-1}\Delta t\|u^{n+\frac12}\|_{\epsilon,0}^2\|\nabla\eta^{n+\frac12}\|^2, \tag{4.13}$$

$$\Delta t\left(D_N^h\overline{u^{n+\frac12}}^h\times\nabla\times\phi_h^{n+\frac12},D_N^h\overline{\phi_h^{n+\frac12}}^h\right)\le C\Delta t\|\nabla D_N^h u^{n+\frac12}\|\,\|\nabla\times\phi_h^{n+\frac12}\|\left\|D_N^h\overline{\phi_h^{n+\frac12}}^h\right\|^{\frac12}\left\|\nabla D_N^h\overline{\phi_h^{n+\frac12}}^h\right\|^{\frac12}$$
$$\le CN^2\Delta t\|u^{n+\frac12}\|_{\epsilon,0}\|\nabla\phi_h^{n+\frac12}\|\,\|\phi_h^{n+\frac12}\|_{E,N}^{\frac12}\|\phi_h^{n+\frac12}\|_{\epsilon,N}^{\frac12}$$
$$\le\frac{\nu\Delta t}{16}\|\phi_h^{n+\frac12}\|_{\epsilon,N}^2+CN^8\,\nu^{-3}\Delta t\|u^{n+\frac12}\|_{\epsilon,0}^4\|\phi_h^{n+\frac12}\|_{E,N}^2, \tag{4.14}$$

$$\Delta t\left(D_N^h\overline{\eta^{n+\frac12}}^h\times\nabla\times\eta^{n+\frac12},D_N^h\overline{\phi_h^{n+\frac12}}^h\right)\le C\Delta t\left\|\nabla D_N^h\overline{\eta^{n+\frac12}}_h\right\|\|\nabla\times\eta^{n+\frac12}\|\left\|\nabla D_N^h\overline{\phi_h^{n+\frac12}}\right\|$$
$$\le\frac{\nu\Delta t}{16}\|\phi_h^{n+\frac12}\|_{\epsilon,N}^2+CN^4\,\nu^{-1}\Delta t\|\eta^{n+\frac12}\|_{\epsilon,0}^2\|\nabla\eta^{n+\frac12}\|^2, \tag{4.15}$$

$$\Delta t\left(D_N^h\overline{\eta^{n+\frac12}}^h\times\nabla\times\phi_h^{n+\frac12},D_N^h\overline{\phi_h^{n+\frac12}}^h\right)\le C\Delta t\|\nabla D_N^h\overline{\eta}^{n+\frac12}{}^h\|\,\|\nabla\phi_h^{n+\frac12}\|\left\|D_N^h\overline{\phi_h^{n+\frac12}}_h\right\|^{\frac12}\left\|\nabla D_N^h\overline{\phi_h^{n+\frac12}}_h\right\|^{\frac12}$$
$$\le\frac{\nu\Delta t}{16}\|\phi_h^{n+\frac12}\|_{\epsilon,N}^2+CN^8\Delta t\,\nu^{-3}\|\eta^{n+\frac12}\|_{\epsilon,0}^4\|\phi_h^{n+\frac12}\|_{E,N}^2, \tag{4.16}$$

$$\Delta t\left(D_N^h\overline{\eta^{n+\frac12}}^h\times\nabla\times u^{n+\frac12},D_N^h\overline{\phi_h^{n+\frac12}}^h\right)\le C\Delta t\|\left\|\nabla D_N^h\overline{\eta^{n+\frac12}}^h\right\|\|\nabla\times u^{n+\frac12}\|\left\|\nabla D_N^h\overline{\phi_h^{n+\frac12}}^h\right\|$$
$$\le\frac{\nu\Delta t}{16}\|\phi_h^{n+\frac12}\|_{\epsilon,N}^2+CN^4\,\nu^{-1}\Delta t\|\eta^{n+\frac12}\|_{\epsilon,0}^2\|\nabla u^{n+\frac12}\|^2. \tag{4.17}$$

https://doi.org/10.1051/m2an/2010042 Published online by Cambridge University Press

Combining (4.10) to (4.17) and summing from $n = 0$ to $M-1$ (assuming that $\|\phi_h^0\| = 0$) reduces (4.9) to

$$\begin{aligned}
&\|\phi_h^M\|_{E,N}^2 + \nu\Delta t \sum_{n=0}^{M-1} \|\phi_h^{n+\frac{1}{2}}\|_{\epsilon,N}^2 \le \Delta t \sum_{n=0}^{M-1} CN^8\,\nu^{-3}(\|u^{n+\frac{1}{2}}\|_{\epsilon,0}^4 + \|\eta^{n+\frac{1}{2}}\|_{\epsilon,0}^4)\,\|\phi_h^{n+\frac{1}{2}}\|_{E,N}^2 \\
&+ \Delta t \sum_{n=0}^{M-1} CN^2(\nu+\gamma+N^2\nu^{-1}\|u^{n+\frac{1}{2}}\|_{\epsilon,0}^2 + N^2\nu^{-1}\|\eta^{n+\frac{1}{2}}\|_{\epsilon,0}^2)\|\nabla\eta^{n+\frac{1}{2}}\|^2 \\
&+ \Delta t \sum_{n=0}^{M-1} CN^4\,\nu^{-1}\|\eta^{n+\frac{1}{2}}\|_{\epsilon,0}^2\,\|\nabla u^{n+\frac{1}{2}}\|^2 \\
&+ \Delta t \sum_{n=0}^{M-1} C(N)\Delta t\gamma^{-1}\|p^{n+\frac{1}{2}} - q\|^2 + \Delta t \sum_{n=0}^{M-1} \left| Intp\left(u^n, p^n; D_N^h \overline{\phi_h^{n+\frac{1}{2}}}^h\right)\right|. \qquad (4.18)
\end{aligned}$$

Now, we continue to bound the terms on the RHS of (4.18). We have that

$$\begin{aligned}
&\Delta t \sum_{n=0}^{M-1} CN^8\,\nu^{-3}(\|u^{n+\frac{1}{2}}\|_{\epsilon,0}^4 + \|\eta^{n+\frac{1}{2}}\|_{\epsilon,0}^4)\,\|\phi_h^{n+\frac{1}{2}}\|_{E,N}^2 \\
&\qquad\qquad \le CN^8\nu^{-3}\Delta t \sum_{n=0}^{M-1} (\|\nabla u^{n+\frac{1}{2}}\|^4 + h^{4k}|u^{n+\frac{1}{2}}|_{k+1}^4)\,\|\phi_h^{n+\frac{1}{2}}\|_{E,N}^2, \qquad (4.19)
\end{aligned}$$

$$\begin{aligned}
&\Delta t \sum_{n=0}^{M-1} CN^2(\nu+\gamma+N^2\nu^{-1}\|u^{n+\frac{1}{2}}\|_{\epsilon,0}^2 + N^2\nu^{-1}\|\eta^{n+\frac{1}{2}}\|_{\epsilon,0}^2)\|\nabla\eta^{n+\frac{1}{2}}\|^2 \le \Delta t CN^2(\nu+\gamma)\sum_{n=0}^{M-1}\|\nabla\eta^n\|^2 \\
&+ CN^4\nu^{-1}\Delta t \sum_{n=0}^{M-1} \left(\|u^{n+\frac{1}{2}}\|_{\epsilon,0}^2 + \|\eta^{n+\frac{1}{2}}\|_{\epsilon,0}^2\right)\left(\|\nabla\eta^n\|^2 + \|\nabla\eta^{n+1}\|^2\right) \\
\le\ & \Delta t CN^2(\nu+\gamma)\sum_{n=0}^{M-1} h^{2k}|u^n|_{k+1}^2 \\
&+ CN^4\nu^{-1}\,h^{2k}\left(\Delta t\sum_{n=0}^{M}|u^n|_{k+1}^4 + \Delta t\sum_{n=0}^{M}\|\nabla u^n\|^4\right) + CN^4\nu^{-1}\,h^{4k}\Delta t\sum_{n=0}^{M}|u^n|_{k+1}^4 \\
\le\ & CN^2(\nu+\gamma)h^{2k}|||u|||_{2,k+1}^2 + CN^4\nu^{-1}\,h^{2k}\left(|||u|||_{4,k+1}^4 + |||\nabla u|||^4\right), \qquad (4.20)
\end{aligned}$$

and similarly,

$$\begin{aligned}
\Delta t \sum_{n=0}^{M-1} CN^4\nu^{-1}\|\eta^{n+\frac{1}{2}}\|_{\epsilon,0}^2\,\|\nabla u^{n+\frac{1}{2}}\|^2 &\le CN^4\nu^{-1}\Delta t\sum_{n=0}^{M-1}\left(\|\eta^n\|_{\epsilon,0}^2 + \|\eta^{n+1}\|_{\epsilon,0}^2\right)\|\nabla u^{n+\frac{1}{2}}\|^2 \\
&\le CN^4\,\nu^{-1}\,h^{2k}\left(\Delta t\sum_{n=0}^{M-1}|u^n|_{k+1}^2\,\|\nabla u^{n+\frac{1}{2}}\|^2 + \Delta t\sum_{n=0}^{M-1}|u^{n+1}|_{k+1}^2\,\|\nabla u^{n+\frac{1}{2}}\|^2\right) \\
&\le CN^4\nu^{-1}\,h^{2k}\left(\Delta t\sum_{n=0}^{M}|u^n|_{k+1}^4 + \Delta t\sum_{n=0}^{M}\|\nabla u^n\|^4\right) \\
&= CN^4\nu^{-1}\,h^{2k}\left(|||u|||_{4,k+1}^4 + |||\nabla u|||^4\right), \qquad (4.21)
\end{aligned}$$

https://doi.org/10.1051/m2an/2010042 Published online by Cambridge University Press

from Lemma 2.12,

$$\begin{aligned}\Delta t\sum_{n=0}^{M-1}C(N)\gamma^{-1}\|p_{n+\frac{1}{2}}-q\|^2 &\le C(N)\gamma^{-1}\Delta t\sum_{n=0}^{M-1}\|p(t_{n+\frac{1}{2}})-q\|^2+\|p_{n+\frac{1}{2}}-p(t_{n+\frac{1}{2}})\|^2\\ &\le C(N)\gamma^{-1}\left(h^{2s+2}\Delta t\sum_{n=0}^{M-1}\|p(t_{n+\frac{1}{2}})\|_{s+1}^2+\Delta t\sum_{n=0}^{M-1}\frac{1}{48}(\Delta t)^3\int_{t_n}^{t_{n+1}}\|p_{tt}\|^2\,\mathrm{d}t\right)\\ &\le C(N)\gamma^{-1}\left(h^{2s+2}|||p_{\frac{1}{2}}|||_{2,s+1}^2+(\Delta t)^4\|p_{tt}\|_{2,0}^2\right).\end{aligned}\tag{4.22}$$

We now bound the terms in $Intp\left(u^n,p^n;D_N^h\overline{\phi_h^{n+\frac{1}{2}}}^h\right)$. Using Cauchy-Schwarz and Young's inequalities, Lemmas 2.12, 2.7 and 2.9,

$$\begin{aligned}\left(\frac{u^{n+1}-u^n}{\Delta t}-u_t(t^{n+\frac{1}{2}}),D_N^h\overline{\phi_h^{n+\frac{1}{2}}}^h\right)&\le\frac{1}{2}\|\phi_h^{n+\frac{1}{2}}\|_{E,N}^2+\frac{N^2}{2}\left\|\frac{u^{n+1}-u^n}{\Delta t}-u_t(t^{n+\frac{1}{2}})\right\|^2\\ &\le\frac{1}{2}\|\phi_h^{n+\frac{1}{2}}\|_{E,N}^2+\frac{N^2}{2}\frac{(\Delta t)^3}{1280}\int_{t^n}^{t^{n+1}}\|u_{ttt}\|^2\,\mathrm{d}t,\end{aligned}\tag{4.23}$$

$$\begin{aligned}\gamma\left(\nabla\cdot(u^{n+\frac{1}{2}}-u(t^{n+\frac{1}{2}})),\nabla\cdot D_N^h\overline{\phi_h^{n+\frac{1}{2}}}^h\right)&\le C\gamma\Delta t\|\nabla\cdot(u^{n+\frac{1}{2}}-u(t^{n+\frac{1}{2}}))\|\left\|\nabla\cdot D_N^h\overline{\phi_h^{n+\frac{1}{2}}}^h\right\|\\ &\le\epsilon_0\nu\|\phi_h^{n+\frac{1}{2}}\|_{\epsilon,N}^2+C(N)\gamma\frac{(\Delta t)^3}{48}\int_{t^n}^{t^{n+\frac{1}{2}}}\|\nabla u_{tt}\|^2\,\mathrm{d}t,\end{aligned}\tag{4.24}$$

$$\begin{aligned}\left(p^{n+\frac{1}{2}}-p(t^{n+\frac{1}{2}}),\nabla\cdot D_N^h\overline{\phi_h^{n+\frac{1}{2}}}^h\right)&\le\epsilon_1\nu\|\phi_h^{n+\frac{1}{2}}\|_{\epsilon,N}^2+C(N)\gamma^{-1}\|p^{n+\frac{1}{2}}-p(t^{n+\frac{1}{2}})\|^2\\ &\le\epsilon_1\nu\|\phi_h^{n+\frac{1}{2}}\|_{\epsilon,N}^2+C(N)\gamma^{-1}\frac{(\Delta t)^3}{48}\int_{t^n}^{t^{n+1}}\|p_{tt}\|^2\,\mathrm{d}t,\end{aligned}\tag{4.25}$$

$$\begin{aligned}\left(f(t^{n+\frac{1}{2}})-f^{n+\frac{1}{2}},D_N^h\overline{\phi_h^{n+\frac{1}{2}}}^h\right)&\le\frac{1}{2}\|\phi_h^{n+\frac{1}{2}}\|_{E,N}^2+\frac{N^2}{2}\|f(t^{n+\frac{1}{2}})-f^{n+\frac{1}{2}}\|^2\\ &\le\frac{1}{2}\|\phi_h^{n+\frac{1}{2}}\|_{E,N}^2+N^2\frac{(\Delta t)^3}{48}\int_{t^n}^{t^{n+1}}\|f_{tt}\|^2\,\mathrm{d}t,\end{aligned}\tag{4.26}$$

$$\begin{aligned}\left(\nabla u^{n+\frac{1}{2}}-\nabla u(t^{n+\frac{1}{2}}),\nabla D_N^h\overline{\phi_h^{n+\frac{1}{2}}}^h\right)&\le\epsilon_2\nu\,\|\phi_h^{n+\frac{1}{2}}\|_{\epsilon,N}^2+CN^2\,\nu\|\nabla u^{n+\frac{1}{2}}-\nabla u(t^{n+\frac{1}{2}})\|^2\\ &\le\epsilon_2\nu\,\|\phi_h^{n+\frac{1}{2}}\|_{\epsilon,N}^2+CN^2\,\nu\frac{(\Delta t)^3}{48}\int_{t^n}^{t^{n+\frac{1}{2}}}\|\nabla u_{tt}\|^2\,\mathrm{d}t,\end{aligned}\tag{4.27}$$

https://doi.org/10.1051/m2an/2010042 Published online by Cambridge University Press

$$
\begin{aligned}
&\left(u^{n+\frac{1}{2}} \times \left(\nabla \times u^{n+\frac{1}{2}}\right), D_N^h \overline{\phi_h^{n+\frac{1}{2}}}^h\right) - \left(u(t^{n+\frac{1}{2}}) \times \left(\nabla \times u(t^{n+\frac{1}{2}})\right), D_N^h \overline{\phi_h^{n+\frac{1}{2}}}^h\right) \\
&= \left((u^{n+\frac{1}{2}} - u(t^{n+\frac{1}{2}})) \times \nabla \times u^{n+\frac{1}{2}}, D_N^h \overline{\phi_h^{n+\frac{1}{2}}}^h\right) + \left(u(t^{n+\frac{1}{2}}) \times \left(\nabla \times (u^{n+\frac{1}{2}} - u(t^{n+\frac{1}{2}}))\right), D_N^h \overline{\phi_h^{n+\frac{1}{2}}}^h\right) \\
&\le CN \|\nabla(u^{n+\frac{1}{2}} - u(t^{n+\frac{1}{2}}))\| \, \|\nabla \phi_h^{n+\frac{1}{2}}\| \left(\|\nabla u^{n+\frac{1}{2}}\| + \|\nabla u(t^{n+\frac{1}{2}})\|\right) \\
&\le CN^2 \nu^{-1} \left(\|\nabla u^{n+\frac{1}{2}}\|^2 + \|\nabla u(t^{n+\frac{1}{2}})\|^2\right) \frac{(\Delta t)^3}{48} \int_{t^n}^{t^{n+1}} \|\nabla u_{tt}\|^2 \, \mathrm{d}t + \epsilon_3 \nu \|\phi_h^{n+\frac{1}{2}}\|_{\epsilon,N}^2 \\
&\le C \frac{N^2}{\nu} \frac{(\Delta t)^3}{48} \left(\int_{t^n}^{t^{n+1}} 2(\|\nabla u^{n+\frac{1}{2}}\|^4 + \|\nabla u(t^{n+\frac{1}{2}})\|^4) \, \mathrm{d}t + \int_{t^n}^{t^{n+1}} \|\nabla u_{tt}\|^4 \, \mathrm{d}t\right) + \epsilon_3 \nu \|\phi_h^{n+\frac{1}{2}}\|_{\epsilon,N}^2 \\
&\le C \frac{N^2}{\nu} (\Delta t)^4 (\|\nabla u^{n+\frac{1}{2}}\|^4 + \|\nabla u(t^{n+\frac{1}{2}})\|^4) + C \frac{N^2}{\nu} (\Delta t)^3 \int_{t^n}^{t^{n+1}} \|\nabla u_{tt}\|^4 \, \mathrm{d}t + \epsilon_3 \nu \|\phi_h^{n+\frac{1}{2}}\|_{\epsilon,N}^2, \qquad (4.28)
\end{aligned}
$$

$$
\begin{aligned}
&\left(\left(u^{n+\frac{1}{2}} - D_N^h \overline{u^{n+\frac{1}{2}}}^h\right) \times \left(\nabla \times u^{n+\frac{1}{2}}\right), D_N^h \overline{\phi_h^{n+\frac{1}{2}}}^h\right) \\
&\le \left\|u^{n+\frac{1}{2}} - D_N^h \overline{u^{n+\frac{1}{2}}}^h\right\| \|\nabla u^{n+\frac{1}{2}}\|_\infty \left\|D_N^h \overline{\phi_h^{n+\frac{1}{2}}}^h\right\| \le CN \left\|u^{n+\frac{1}{2}} - D_N^h \overline{u^{n+\frac{1}{2}}}^h\right\| \|\phi_h^{n+\frac{1}{2}}\|_{\epsilon,N} \\
&\le \epsilon_4 \nu \|\phi_h^{n+\frac{1}{2}}\|_{\epsilon,N}^2 + CN^2 \nu^{-1} \left\|u^{n+\frac{1}{2}} - D_N^h \overline{u^{n+\frac{1}{2}}}^h\right\|^2 \\
&\le \epsilon_4 \nu \|\phi_h^{n+\frac{1}{2}}\|_{\epsilon,N}^2 + CN^2 \nu^{-1} \alpha^{4N+4} \|\Delta^{N+1} F^{N+1} u^{n+\frac{1}{2}}\|^2 \qquad (4.29) \\
&\quad + CN^2 \nu^{-1} \left(\frac{\alpha^2 \gamma}{\nu} h^{2k} + \alpha^2 h^{2k} + h^{2k+2} + \frac{\alpha^2 \gamma}{\nu} h^{2k}\right) \left(\sum_{l=0}^{N} \left| F^l \overline{u^{n+\frac{1}{2}}} \right|_{k+1}^2\right).
\end{aligned}
$$

Combine (4.23)–(4.29) to obtain

$$
\begin{aligned}
&\Delta t \sum_{n=0}^{M-1} |Intp\left(u^n, p^n; D_N^h \overline{\phi_h^{n+\frac{1}{2}}}^h\right) \\
&\le \Delta t \sum_{n=0}^{M-1} \|\phi_h^{n+\frac{1}{2}}\|_{E,N}^2 + \Delta t \, (\epsilon_0 + \epsilon_1 + \epsilon_2 + \epsilon_3 + \epsilon_4) \sum_{n=0}^{M-1} \nu \|\phi_h^{n+\frac{1}{2}}\|_{\epsilon,N}^2 \\
&\quad + CN^2 \nu^{-1} \alpha^{4N+4} |||\Delta^{N+1} F^{N+1} u_{\frac{1}{2}}|||_{2,0}^2 \\
&\quad + CN^2 \nu^{-1} h^{2k} \left(\frac{\alpha^2 \gamma}{\nu} + \alpha^2 + h^2 + \frac{\alpha^2 \gamma}{\nu}\right) \left(\sum_{l=0}^{N} ||| \, F^l \, \overline{u}_{\frac{1}{2}} \, |||_{2,k+1}^2\right) \\
&\quad + CN^2 (\Delta t)^4 \left(\|u_{ttt}\|_{2,0}^2 + \nu^{-1} \|p_{tt}\|_{2,0}^2 + \|f_{tt}\|_{2,0}^2 + (\nu + \nu^{-1} \gamma^2) \|\nabla u_{tt}\|_{2,0}^2 + \nu^{-1} \|\nabla u_{tt}\|_{4,0}^4 \right. \\
&\quad \left. + \nu^{-1} |||\nabla u|||_{4,0}^4 + \nu^{-1} |||\nabla u_{\frac{1}{2}}|||_{4,0}^4\right). \qquad (4.30)
\end{aligned}
$$

https://doi.org/10.1051/m2an/2010042 Published online by Cambridge University Press

Let $\epsilon_0 = \epsilon_1 = \epsilon_2 = \epsilon_3 = \epsilon_4 = 1/10$ and with (4.19)–(4.22), (4.30), from (4.18), and using the assumption on γ, we obtain

$$\begin{aligned}
&\|\phi_h^M\|_{E,N}^2 + \nu\Delta t \sum_{n=0}^{M-1} \|\phi_h^{n+\frac{1}{2}}\|_{\epsilon,N}^2 \\
&\qquad \le \Delta t \sum_{n=0}^{M-1} C(N^8\nu^{-3}(\|\nabla u^{n+\frac{1}{2}}\|^4 + h^{4k}|u^{n+\frac{1}{2}}|_{k+1}^4) + 1)\, \|\phi_h^{n+\frac{1}{2}}\|_{E,N}^2 \\
&\qquad\quad + CN^2(\nu+\gamma)h^{2k}|||u|||_{2,k+1}^2 + CN^2\nu^{-1}\, h^{2k}\left(|||u|||_{4,k+1}^4 + |||\nabla u|||_{2,0}^4\right) \\
&\qquad\quad + C(N)\gamma^{-1}h^{2s+2}|||p_{\frac{1}{2}}|||_{2,s+1}^2 + CN^2\nu^{-1}\alpha^{4N+4}|||\Delta^{N+1}F^{N+1}u_{\frac{1}{2}}|||_{2,0}^2 \\
&\qquad\quad + CN^2\nu^{-1}h^{2k}\left(\frac{\alpha^2\gamma}{\nu} + \alpha^2 + h^2 + \frac{\alpha^2\gamma}{\nu}\right)\left(\sum_{l=0}^{N} |||\, F^l\, \overline{u}_{\frac{1}{2}}\, |||_{2,k+1}^2\right) \\
&\qquad\quad + CN^2(\Delta t)^4\Big(\|u_{ttt}\|_{2,0}^2 + \nu^{-1}\|p_{tt}\|_{2,0}^2 + \|f_{tt}\|_{2,0}^2 + (\nu+\nu^{-1}\gamma^2)\|\nabla u_{tt}\|_{2,0}^2 \\
&\qquad\quad + \nu^{-1}\|\nabla u_{tt}\|_{4,0}^4 + \nu^{-1}|||\nabla u|||_{4,0}^4 + \nu^{-1}|||\nabla u_{\frac{1}{2}}|||_{4,0}^4\Big).
\end{aligned} \tag{4.31}$$

Hence, with Δt sufficiently small, *i.e.* $\Delta t < C(N^8\nu^{-3}(|||\nabla u|||_\infty^4 + h^{4k}|||u|||_{\infty,k+1}^4) + 1)^{-1}$, from the discrete Gronwall's Lemma we have

$$\begin{aligned}
&\|\phi_M^h\|^2 + \nu\Delta t \sum_{n=0}^{M-1} \|\nabla\phi_{n+\frac{1}{2}}^h\|^2 \\
&\qquad \le C^*\Big\{CN^2(\nu+\gamma)h^{2k}|||u|||_{2,k+1}^2 + CN^2\nu^{-1}\, h^{2k}\left(|||u|||_{4,k+1}^4 + |||\nabla u|||_{2,0}^4\right) \\
&\qquad\quad + C(N)\gamma^{-1}h^{2s+2}|||p_{\frac{1}{2}}|||_{2,s+1}^2 + CN^2\nu^{-1}\alpha^{4N+4}|||\Delta^{N+1}F^{N+1}u_{\frac{1}{2}}|||_{2,0}^2 \\
&\qquad\quad + CN^2\nu^{-1}h^{2k}\left(\frac{\alpha^2\gamma}{\nu} + \alpha^2 + h^2 + \frac{\alpha^2\gamma}{\nu}\right)\left(\sum_{l=0}^{N} |||\, F^l\, \overline{u}_{\frac{1}{2}}\, |||_{2,k+1}^2\right) \\
&\qquad\quad + CN^2(\Delta t)^4\Big(\|u_{ttt}\|_{2,0}^2 + \nu^{-1}\|p_{tt}\|_{2,0}^2 + \|f_{tt}\|_{2,0}^2 + (\nu+\nu^{-1}\gamma^2)\|\nabla u_{tt}\|_{2,0}^2 \\
&\qquad\quad + \nu^{-1}\|\nabla u_{tt}\|_{4,0}^4 + \nu^{-1}|||\nabla u|||_{4,0}^4 + \nu^{-1}|||\nabla u_{\frac{1}{2}}|||_{4,0}^4\Big)\Big\}
\end{aligned} \tag{4.32}$$

where $C^* = C\exp(C\nu^{-1}T)$.

Estimates (4.1) and (4.2) then follow from the triangle inequality and (4.32). □

5. Numerical experiments

In this section, we provide several examples to demonstrate the effectiveness of the proposed scheme for computing accurate approximations to a variety of fluid flow problems. We study four problems: Green-Taylor vortices, flow over a 2D and 3D step, and the 3d Ethier-Steinman problem. We find that the modified grad-div stabilized scheme with deconvolution for NS-α shows very good accuracy in each of these problems. Moreover, we find it is the combination of these two numerical "fixes", and not either one individually, that provides for such high accuracy.

https://doi.org/10.1051/m2an/2010042 Published online by Cambridge University Press

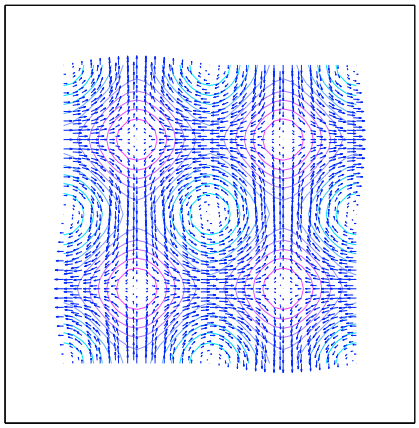


FIGURE 1. The velocity field and pressure contours of the Taylor-Green vortex decay problem at $t = 0$.

5.1. **Numerical experiment 1: Green-Taylor vortices with $\nu = 0.1$**

Our first numerical experiment is to test the theoretically predicted convergence rates. For that, we choose the Green-Taylor vortex decay problem [23,52]. It is an interesting test problem in which the true solution is known, and was used as a numerical test in Chorin [13], Tafti [51] and John and Layton [28].

The prescribed NSE solution in $\Omega = (0,1) \times (0,1)$ has the form

$$\begin{aligned} u_1(x,y,t) &= -\cos(n\pi x)\sin(n\pi y)\mathrm{e}^{-2n^2\pi^2 t/\tau} \\ u_2(x,y,t) &= \sin(n\pi x)\cos(n\pi y)\mathrm{e}^{-2n^2\pi^2 t/\tau} \\ p(x,y,t) &= -\frac{1}{4}(\cos(2n\pi x) + \cos(2n\pi y))\mathrm{e}^{-2n^2\pi^2 t/\tau}. \end{aligned}$$

The pressure p is given here in its usual form. To recover the Bernoulli pressure, compute $P = p + \frac{1}{2}|u|^2$. Note it is the Bernoulli pressure that gets computed in the scheme proposed herein.

When the relaxation time $\tau = Re := \frac{1}{\nu}$, this is a solution of the NSE with $f = 0$, consisting of an $n \times n$ array of oppositely signed vortices that decay as $t \to \infty$. Figure 1 shows the velocity field and pressure contours for the test problem, with $n = 2$.

For this experiment, we choose $Re = 10$, $h = \left\{\frac{1}{4}, \frac{1}{8}, \frac{1}{12}, \frac{1}{16}, \frac{1}{24}\right\}$, $\Delta t \approx h^{3/2}$ using (P_3, P_2) elements. We consider approximations for four cases of parameter choices: usual NS-α ($\gamma = 0$, $N = 0$), with modified grad-div stabilization only ($\gamma = 1$, $N = 0$), with order 1 deconvolution only ($\gamma = 0$, $N = 1$), and NS-α with both the modified grad-div stabilization and order 1 van Cittert approximate deconvolution ($\gamma = 1$, $N = 1$). The $L^2(0, 0.5; H^1(\Omega))$ errors and convergence rates are given in Table 1. These results verify our predicted convergence rates for (P_3, P_2) elements when $\Delta t \leq h^{3/2}$: the $L^2(0, 0.5; H^1(\Omega))$ convergence will be $O(h^{2N+2} + h^3)$. That is, provided a smooth solution, the $N = 1$ schemes will converge to the NSE solution faster than the $N = 0$ scheme, and thus the $N = 1$ scheme can be expected to be more accurate in smooth flow regions. Moreover, this means that even for smooth flows, one cannot expect error from the $N = 0$ schemes to be any better than $O(h^2)$. At such a small Reynolds number, we see grad-div stabilization can have a slight negative effect on error on very coarse meshes, from introducing consistency error. On the finer (although still quite coarse) meshes, this effect is negligible.

https://doi.org/10.1051/m2an/2010042 Published online by Cambridge University Press

TABLE 1. $L^2(0, 0.5, H^1(\Omega))$ errors and convergence rates for approximating solutions when $Re = 10$, for the grad-div modified scheme for NS-α with approximate deconvolution.

	$\frac{\gamma=0}{N=0}$	$\frac{\gamma=0}{N=0}$	$\frac{\gamma=1}{N=0}$	$\frac{\gamma=1}{N=0}$	$\frac{\gamma=0}{N=1}$	$\frac{\gamma=0}{N=1}$	$\frac{\gamma=1}{N=1}$	$\frac{\gamma=1}{N=1}$
h	$\|u-u^h\|_{2,1}$	Rate	$\|u-u^h\|_{2,1}$	Rate	$\|u-u^h\|_{2,1}$	Rate	$\|u-u^h\|_{2,1}$	Rate
1/4	0.2065		0.3682		0.1928		0.3612	
1/8	0.0593	1.80	0.0535	2.78	0.0357	2.56	0.0411	3.14
1/12	0.0222	2.42	0.0227	2.11	0.0061	4.36	0.0076	4.16
1/16	0.0129	1.89	0.0130	1.94	0.0030	2.47	0.0035	2.70
1/24	0.0055	2.10	0.0055	2.12	0.0010	2.71	0.0011	2.85

TABLE 2. $L^\infty(0, 0.5, L^2(\Omega))$ errors for approximations when $Re = 10\,000$, for the grad-div modified scheme for NS-α with approximate deconvolution.

	$\gamma = N = 0$	$\gamma = 1,\ N = 0$	$\gamma = 0,\ N = 1$	$\gamma = N = 1$
h	$\|\|\|u-u^h\|\|\|_{\infty,0}$	$\|\|\|u-u^h\|\|\|_{\infty,0}$	$\|\|\|u-u^h\|\|\|_{\infty,0}$	$\|\|\|u-u^h\|\|\|_{\infty,0}$
1/4	0.4564	0.3145	0.3848	0.2449
1/8	0.3389	0.1801	0.2689	2.05
1/12	0.1852	0.0847	0.1546	0.0110
1/16	0.0885	0.0489	0.0583	0.0038
1/24	0.0276	0.0192	0.0123	0.0026

TABLE 3. $L^2(0, 0.5, H^1(\Omega))$ errors and convergence rates for approximating solutions when $Re = 10\,000$, for the grad-div modified scheme for NS-α with approximate deconvolution.

	$\gamma = N = 0$	$\gamma = 1,\ N = 0$	$\gamma = 0,\ N = 1$	$\gamma = N = 1$
h	$\|\|\|u-u^h\|\|\|_{2,1}$	$\|\|\|u-u^h\|\|\|_{2,1}$	$\|\|\|u-u^h\|\|\|_{2,1}$	$\|\|\|u-u^h\|\|\|_{2,1}$
1/4	6.8575	4.0065	6.2504	3.2493
1/8	10.3975	3.3753	9.1907	1.2740
1/12	7.8530	2.2385	7.1056	0.3691
1/16	4.9461	1.5756	3.8409	0.1912
1/24	2.1009	0.7727	1.3455	0.1246

5.2. **Numerical experiment 2: Green-Taylor vortices with $\nu = 0.0001$**

We now test the errors if we change numerical experiment 1 with one modification: set $\nu = 0.0001$ (*i.e.* set the Reynolds number to 10 000). Results are shown in Tables 2 and 3, as $L^\infty(0, 0.5; L^2(\Omega))$ and $L^2(0, 0.5; H^1(\Omega))$ errors. In both tables, it is clear that the the addition of the modified grad-div stabilization and deconvolution each individually improve error *versus* the usual NS-α scheme, but it is the combination of modified grad-div stabilization and deconvolution ($\gamma = 1,\ N = 1$) that gives the best results.

5.3. **Experiment 3: the Ethier-Steinman problem**

The next numerical experiment we consider is for computing approximations to the Ethier-Steinman exact Navier-Stokes solution from [17] on $[-1, 1]^3$. For chosen parameters a, d and viscosity ν, their exact NSE solution

https://doi.org/10.1051/m2an/2010042 Published online by Cambridge University Press

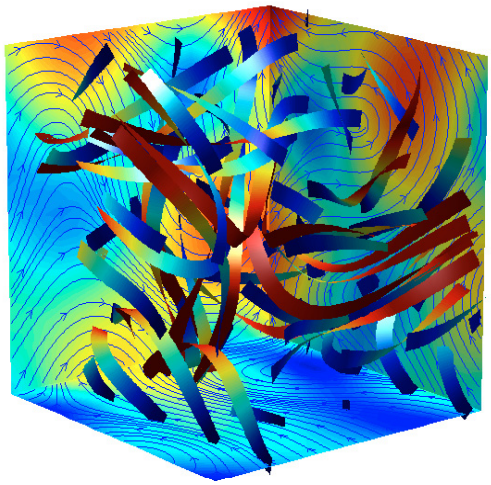


FIGURE 2. The velocity solution to the Ethier-Steinman problem with $a = 1.25$, $d = 1$ at $t = 0$ on the $(-1, 1)^3$ domain. The complex flow structure is seen in the streamribbons in the box and the velocity streamlines and speed contours on the sides.

is given by

$$u_1 = -a\left(\mathrm{e}^{ax}\sin(ay+\mathrm{d}z)+\mathrm{e}^{az}\cos(ax+\mathrm{d}y)\right)\mathrm{e}^{-\nu \mathrm{d}^2 t} \tag{5.1}$$

$$u_2 = -a\left(\mathrm{e}^{ay}\sin(az+\mathrm{d}x)+\mathrm{e}^{ax}\cos(ay+\mathrm{d}z)\right)\mathrm{e}^{-\nu \mathrm{d}^2 t} \tag{5.2}$$

$$u_3 = -a\left(\mathrm{e}^{az}\sin(ax+\mathrm{d}y)+\mathrm{e}^{ay}\cos(az+\mathrm{d}x)\right)\mathrm{e}^{-\nu \mathrm{d}^2 t} \tag{5.3}$$

$$\begin{aligned} p = & -\frac{a^2}{2}(\mathrm{e}^{2ax}+\mathrm{e}^{2ay}+\mathrm{e}^{2az}+2\sin(ax+\mathrm{d}y)\cos(az+\mathrm{d}x)\mathrm{e}^{a(y+z)} \\ & +2\sin(ay+\mathrm{d}z)\cos(ax+\mathrm{d}y)\mathrm{e}^{a(z+x)} \\ & +2\sin(az+\mathrm{d}x)\cos(ay+\mathrm{d}z)\mathrm{e}^{a(x+y)})\mathrm{e}^{-\nu \mathrm{d}^2 t}. \end{aligned} \tag{5.4}$$

Again we give the pressure in its usual form, although our scheme indeed approximates instead the Bernoulli pressure $P = p + \frac{1}{2}|u|^2$.

This problem was developed as a 3d analogue to the Taylor vortex problem, for the purpose of benchmarking. Although unlikely to be physically realized, it is a good test problem because it is not only an exact NSE solution, but also it has non-trivial helicity which implies the existence of turbulent structure [40] in the velocity field. The $t = 0$ solution for $a = 1.25$ and $d = 1$ is illustrated in Figure 2.

We compute approximations to (5.1)–(5.4) with $a = 1.25$, $d = 1$, viscosity $\nu = 0.0001$, timestep $\Delta t = 0.01$, endtime $T = 1$, and initial velocity $u^0 = (u_1(0), u_2(0), u_3(0))^T$, using Algorithm 3.1 with 3072 (P_2, P_1) tetrahedral elements, enforcing Dirichlet boundary conditions (from (5.1)–(5.3) on the sides of the box). We compute four cases, to compare results with and without the modified grad-div stabilization and approximate deconvolution $(\gamma, N = 0, 1)$. Note that with given small $\nu = 0.0001$ the solution changes only slightly on the time interval $[0, 1]$.

The results of this experiment are displayed in Figure 3 in a plot of the approximated solutions' relative $L^2(\Omega)$ error *versus* time. The superiority of the approximated solutions computed with the modified grad-div

https://doi.org/10.1051/m2an/2010042 Published online by Cambridge University Press

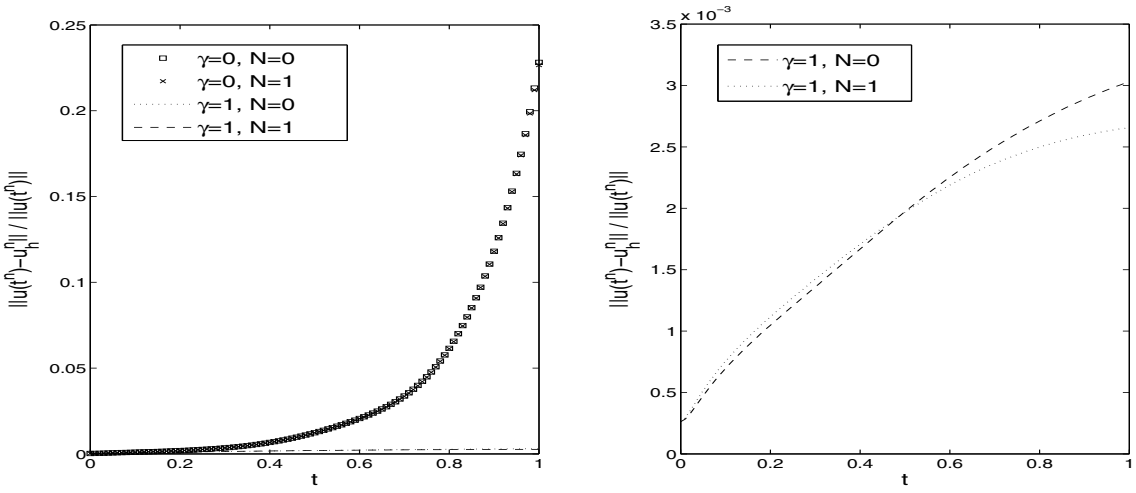


FIGURE 3. Relative L^2 error *vs.* time in the numerical scheme for NS-α studied herein, for the Ethier-Steinman problem with $a = 1.25,\ d = 1,\ Re = 10\,000$, $\Delta t = 0.01$, with varying γ and N. The left plot shows the error from four schemes, but since the error when ($\gamma = 0, N = 0$ or 1) is so large, comparing the ($\gamma = 1, N = 0$) and ($\gamma = 1, N = 1$) schemes was impossible due to scaling. The plot on the right is thus the same plot, but without the error from the $\gamma = 0$ schemes.

stabilization is evident from Figure 3, as we see from the plot on the left that when $\gamma = 0$, relative L^2 error grows exponentially fast with time, while by comparison relative errors in the ($\gamma = 1, N = 0$) and ($\gamma = 1, N = 1$) schemes are very small in comparison. The plot on the right is the same as the left plot, except that the $\gamma = 0$ plots are removed, allowing a comparison of the $\gamma = 1$ schemes. From this we see how deconvolution adds accuracy. Its effect appears more pronounced with later times, and it appears that if we continued the simulations, its effect would be even greater.

5.4. **Numerical experiment 4: flow over a step**

This numerical experiment shows the effectiveness of adding the modified grad-div stabilization and deconvolution to NS-α by testing it on the benchmark problem of flow over a forward and backward facing step. The domain Ω is a 40×10 rectangle with a 1×1 step 5 units into the channel at the bottom. The top and bottom of the channel as well as the step are prescribed with no-slip boundary conditions, and the sides are given the parabolic profile $(y(10 - y)/25, 0)^{\mathrm{T}}$. We use the initial condition of $u_0 = (y(10 - y)/25, 0)^{\mathrm{T}}$ inside Ω, and run the test to $T = 40$ using timestep $\Delta t = 0.01$. For a chosen viscosity $\nu = 1/600$, it is known that the correct behavior is for an eddy to form behind the step, grow, detach from the step to move down the channel, and a new eddy forms. For a more detailed description of the problem, see [25] or [28].

The eddy formation and separation present in this test problem is part of a complex flow structure, and its capture is critical for an effective fluid model. Moreover, a useful fluid model will correctly predict this behavior on a coarser mesh than a NSE direct numerical simulation could. We compute using Algorithm 3.1 with (P_3, P_2) triangular elements on two meshes, a coarse mesh yielding 5091 degrees of freedom and a finer mesh with 8927 degrees of freedom.

Figures 4 and 5 show the solution of the NSE computed directly on the coarse and finer meshes respectively, each using the skew-symmetric form of the nonlinearity (thus avoiding the larger error associated with Bernoulli pressures in the rotational form of the nonlinearity [33]). Figure 4 shows that the direct computation of the NSE on the coarse mesh is under-resolved; although an eddy forms and detaches, oscillations become present

https://doi.org/10.1051/m2an/2010042 Published online by Cambridge University Press

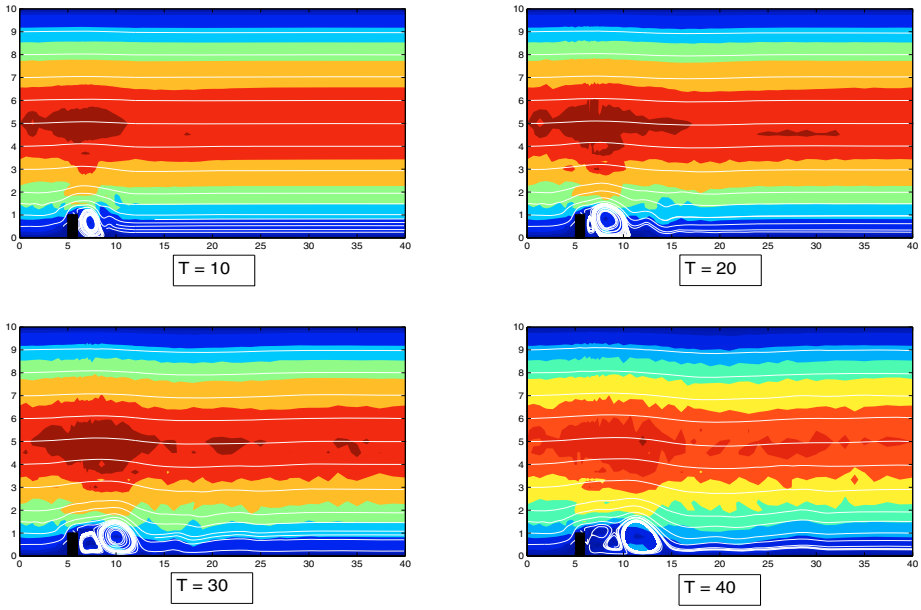


FIGURE 4. The above figure shows the velocity streamlines and speed contours for the coarse mesh solution of the NSE with the skew-symmetric form of the nonlinearity. Shown is the solution at $T = 10$, 20, 30 and 40, which is under-resolved, as evidenced by the oscillations in the speed contours.

in the solution by $T = 10$, and by $T = 40$ have accumulated enough to destroy the solution. From Figure 5, we observe that the NSE is fully resolved on fine mesh, and captures eddy generation and separation behind the step while maintaining a smooth flow structure. These plots match the solution found in [25,28,32], and thus we take it as the "truth" solution.

Figure 6 shows the coarse mesh solution for NS-α at $\alpha = 0.25$ (for the coarse mesh, $h \approx 0.25$) and without any stabilization or deconvolution ($\gamma = N = 0$). The $\alpha = 0.25$ solution does predict eddy detachment and reformation, but has oscillations that have grown to create a very bad solution; this computation was clearly under-resolved. Increasing the regularization parameter was found to suppress oscillations from destroying the solution, but prevents the detachment of the eddy from the step; increasing N also showed only slight improvement over the $N = 0$ solution, and so we omit showing these results. We note this is consistent with our hypothesis about the base model: since the pressure in this flow will have boundary layer effects, it will be complex and thus will be the dominant source of error. Increasing the order of deconvolution reduces the consistency error created by the regularization in the nonlinearity, and thus will have a negligible effect on reducing velocity error when the pressure error's effect is dominant. Hence the NS-α scheme, even with deconvolution, does not give an accurate approximation when computed on the coarser mesh when $\gamma = 0$.

Figures 7 and 8 show the coarse mesh solutions to the NS-α scheme again with $\alpha = 0.25$, $N = 0$ and $N = 1$ respectively, but *with the modified grad-div stabilization added*: $\gamma = 1$ in Algorithm 3.1. The stabilization completely eliminates the oscillations present in Figure 6, correctly predicts eddy formation and detachment, and gives streamlines and speed contours that agree well with those of the truth solution in both the $N = 0$ and $N = 1$ cases. However, the $N = 1$ is visibly a better match to the true solution at both $T = 30$ and $T = 40$.

https://doi.org/10.1051/m2an/2010042 Published online by Cambridge University Press

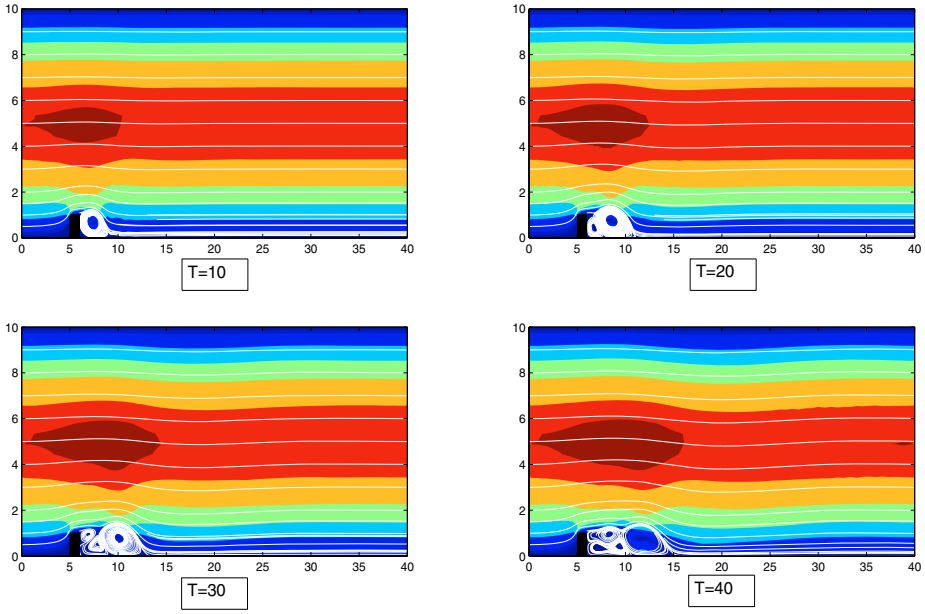


FIGURE 5. The above figure shows the velocity streamlines and speed contours for the NSE at $T = 10$, 20, 30 and 40 on the finer mesh. This is the "truth" solution for the test problem.

5.5. **Numerical experiment 5: 3D flow over a step**

Our final experiment is for 3D flow over a step. The problem setup is similar to the 2D step, and is taken from [29]. The domain is a $10 \times 40 \times 10$ rectangular box, with a step of height 1 and width 1 set at the bottom of the channel, starting 5 units in. No slip boundary conditions are prescribed on the top, bottom, front and back of the box as well as on the step. The constant inflow profile of $u = \langle 0, 1, 0 \rangle$ is used as a Dirichlet condition for the inflow. Since the model studied herein is in rotational form, the so-called do-nothing boundary condition (which corresponds to zero traction) is inappropriate, and so the advective boundary condition is used. As in [29], we use the steady NSE solution with $Re = 20$ as the initial condition, and compute to $T = 20$ using $\nu = 1/200$, giving the Reynolds number $Re = 200$, using the size of the step for the length scale.

Results were computed using (P_3, P_2) Taylor-Hood elements on a coarse tetrahedral mesh providing 7842 velocity degrees of freedom, with a timestep of $\Delta t = 0.01$. Simulations were run with $\gamma = N = 0$, $\gamma = 1$, $N = 0$, and $\gamma = N = 1$, and $\alpha = 1$. The plot of the $x = 5$ midplane's velocity streamlines and speed contours at $T = 20$ for $\gamma = N = 0$ is shown in Figure 9, and is clearly incorrect. The streamlines indicate significant oscillations are present, and by examining the scale of the speed contours it is clear the solution is non-physical. For the solutions with $\gamma = 1$, however, we see much better results. The plot for the $\gamma = 1$, $N = 0$ solution is shown in Figure 10; the plot for $\gamma = N = 1$ is visually identical, and so is omitted. The speed contours and streamlines show a relatively smooth flow is obtained, and recirculation after the step is found. On this coarse mesh, not every detail of the flow can be resolved. However, this experiment does show that the stabilized method can be effective at finding flow averages on coarse meshes, whereas the unstabilized method can be unstable.

https://doi.org/10.1051/m2an/2010042 Published online by Cambridge University Press

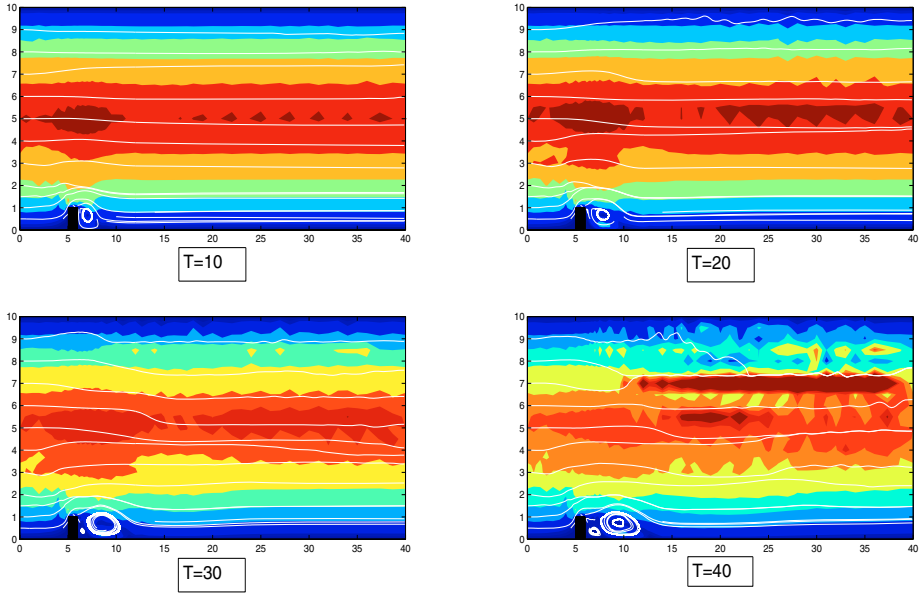


FIGURE 6. The above figure shows the velocity streamlines and speed contours for the coarse mesh solution of NS-α with $\alpha = 0.25$, $\gamma = N = 0$. Shown is the solution at $T = 10$, 20, 30 and 40, which shows eddy formation and detachment, but reveals the flow is very under-resolved, as evidenced by the oscillations in the speed contours.

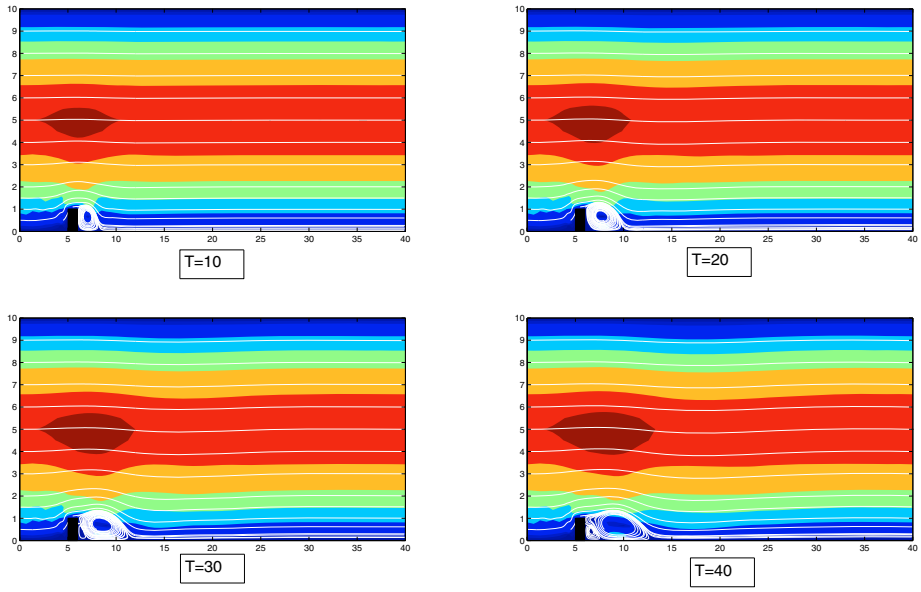


FIGURE 7. The above figure shows the velocity streamlines and speed contours for the coarse mesh solution of NS-α with $\alpha = 0.25$, $\gamma = 1$ and $N = 0$. Shown is the solution at $T = 10$, 20, 30 and 40, which shows eddy formation and detachment, and a smooth resolved flow.

https://doi.org/10.1051/m2an/2010042 Published online by Cambridge University Press

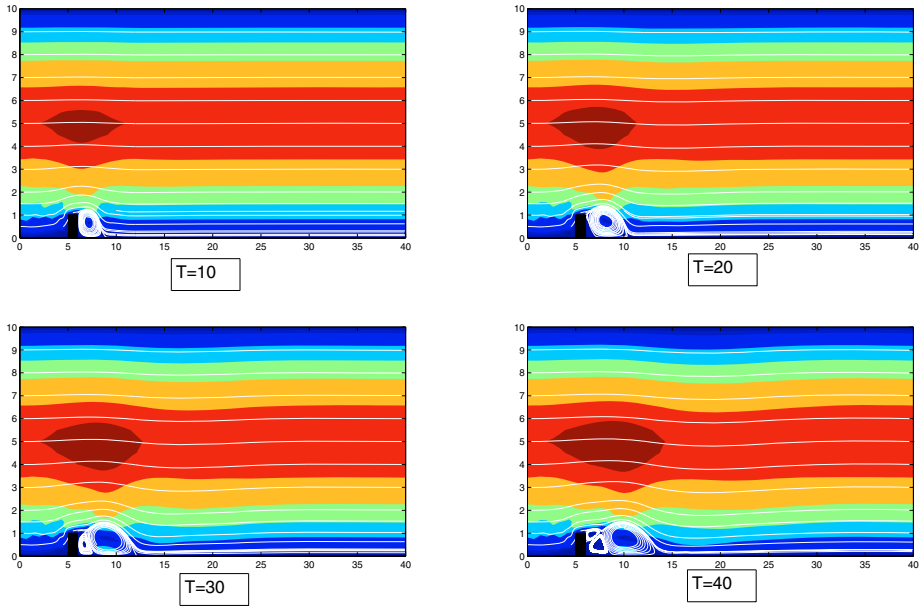


FIGURE 8. The above figure shows the velocity streamlines and speed contours for the coarse mesh solution of NS-α with $\alpha = 0.25$, $\gamma = 1$ and $N = 1$. Shown is the solution at $T = 10, 20, 30$ and 40, which shows eddy formation and detachment, and a smooth resolved flow that matches the truth solution well.

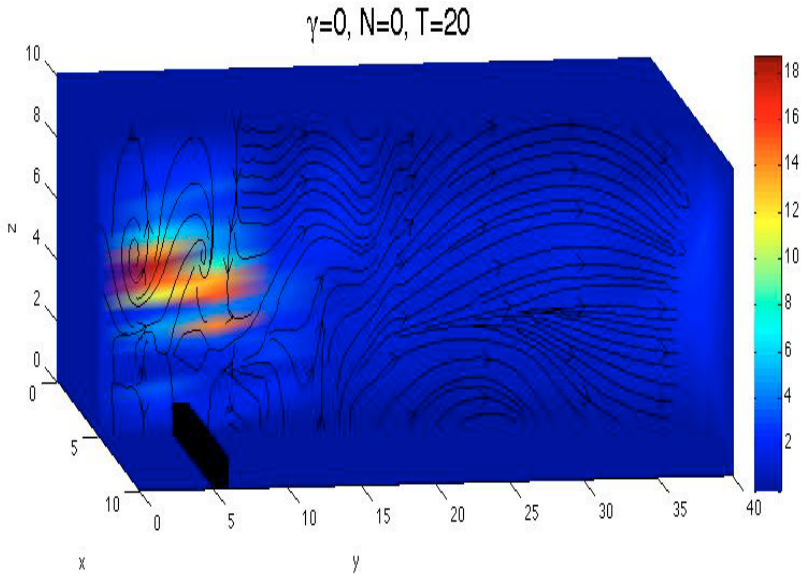


FIGURE 9. Shown above is the speed contours and velocity streamlines at $T = 20$ for the NS-α ($\gamma = N = 0$) simulation of experiment 5. This solution is very poor.

https://doi.org/10.1051/m2an/2010042 Published online by Cambridge University Press

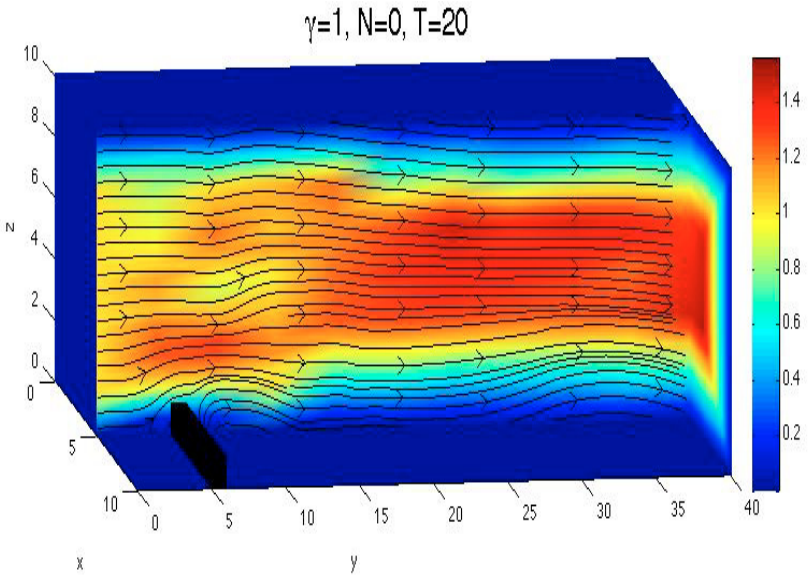


FIGURE 10. Shown above is the speed contours and velocity streamlines at $T = 20$ for the NS-α with stabilization ($\gamma = 1$) simulation of experiment 5. This solution is much better than for the unstabilized simulation.

6. Conclusions

We have proposed and analyzed a FEM scheme for NS-α that combines the model with the carefully derived combination of a stabilization of grad-div type and an adapted approximate deconvolution of the (modified) filtering. The scheme "fixes" two major sources of error, consistency error of the model and the negative influence of the Bernoulli type of pressure on the velocity error, that arise in FEM computations of NS-α, and thus provides for accurate and reliable computations with NS-α. Through a delicate analysis, we prove the scheme is both stable and optimally convergent, and that the grad-div type stabilization reduces the effect of the pressure error on the velocity error. Finally numerical experiments were given that demonstrate a dramatic improvement of the proposed scheme over the standard scheme, with only approximate deconvolution and grad-div stabilization individually and with both of them.

References

[1] N.A. Adams and S. Stolz, On the approximate deconvolution procedure for LES. *Phys. Fluids* **2** (1999) 1699–1701.
[2] N.A. Adams and S. Stolz, *Deconvolution methods for subgrid-scale approximation in large eddy simulation*, *Modern Simulation Strategies for Turbulent Flow*. R.T. Edwards (2001).
[3] G. Baker, *Galerkin approximations for the Navier-Stokes equations*. Harvard University (1976).
[4] J.J. Bardina, H. Ferziger and W.C. Reynolds, *Improved subgrid scale models for large eddy simulation*. AIAA Pap. (1983).
[5] L.C. Berselli, T. Iliescu and W.J. Layton, *Mathematics of Large Eddy Simulation of Turbulent Flows*, *Scientific Computation*. Springer (2006).
[6] S. Brenner and L.R. Scott, *The Mathematical Theory of Finite Element Methods*. Springer-Verlag (1994).
[7] E. Burman, Pressure projection stabilizations for Galerkin approximations of Stokes' and Darcy's problem. *Numer. Methods Partial Differ. Equ.* **24** (2008) 127–143.
[8] E. Burman and A. Linke, Stabilized finite element schemes for incompressible flow using Scott-Vogelius elements. *Appl. Num. Math.* **58** (2008) 1704–1719.
[9] R. Camassa and D. Holm, An integrable shallow water equation with peaked solutions. *Phys. Rev. Lett.* **71** (1993) 1661–1664.

https://doi.org/10.1051/m2an/2010042 Published online by Cambridge University Press

[10] S. Chen, C. Foias, D. Holm, E. Olson, E. Titi and S. Wynne, The Camassa-Holm equations as a closure model for turbulent channel and pipe flow. *Phys. Rev. Lett.* **81** (1998) 5338–5341.
[11] S. Chen, C. Foias, D. Holm, E. Olson, E. Titi and S. Wynne, The Camassa-Holm equations and turbulence. *Physica D* **133** (1999) 49–65.
[12] S. Chen, D. Holm, L. Margolin and R. Zhang, Direct numerical simulations of the Navier-Stokes alpha model. *Physica D* **133** (1999) 66–83.
[13] A.J. Chorin, Numerical solution for the Navier-Stokes equations. *Math. Comp.* **22** (1968) 745–762.
[14] B. Cockburn, G. Kanschat and D. Schotzau, A locally conservative LDG method for the incompressible Navier-Stokes equations. *Math. Comp.* **74** (2005) 1067–1095.
[15] R. Codina, Stabilized finite element approximation of transient incompressible flows using orthogonal subscales. *Comput. Methods Appl. Mech. Engrg.* **191** (2002) 4295–4321.
[16] J. Connors, Convergence analysis and computational testing of the finite element discretization of the Navier-Stokes-alpha model. *Numer. Methods Partial Differ. Equ.* (to appear).
[17] C. Ethier and D. Steinman, Exact fully 3d Navier-Stokes solutions for benchmarking. *Int. J. Numer. Methods Fluids* **19** (1994) 369–375.
[18] L.P. Franca and S.L. Frey, Stabilized finite element methods. II. The incompressible Navier-Stokes equations. *Comput. Methods Appl. Mech. Engrg.* **99** (1992) 209–233.
[19] C. Foias, D. Holm and E. Titi, The Navier-Stokes-alpha model of fluid turbulence. *Physica D* **152-153** (2001) 505–519.
[20] C. Foias, D. Holm and E. Titi, The three dimensional viscous Camassa-Holm equations, and their relation to the Navier-Stokes equations and turbulence theory. *J. Dyn. Diff. Equ.* **14** (2002) 1–35.
[21] T. Gelhard, G. Lube, M.A. Olshanskii and J.-H. Starcke, Stabilized finite element schemes with LBB-stable elements for incompressible flows. *J. Comput. Appl. Math.* **177** (2005) 243–267.
[22] V. Gravemeier, W.A. Wall and E. Ramm, Large eddy simulation of turbulent incompressible flows by a three-level finite element method. *Int. J. Numer. Methods Fluids* **48** (2005) 1067–1099.
[23] A.E. Green and G.I. Taylor, Mechanism of the production of small eddies from larger ones. *Proc. Royal Soc. A* **158** (1937) 499–521.
[24] J.L. Guermond, J.T. Oden and S. Prudhomme, An interpretation of the Navier-Stokes-alpha model as a frame-indifferent Leray regularization. *Physica D* **177** (2003) 23–30.
[25] M. Gunzburger, *Finite Element Methods for Viscous Incompressible Flow: A Guide to Theory, Practice, and Algorithms*. Academic Press, Boston (1989).
[26] P. Hansbo and A. Szepessy, A velocity-pressure streamline diffusion method for the incompressible Navier-Stokes equations. *Comput. Methods Appl. Mech. Engrg.* **84** (1990) 175–192.
[27] V. John and A. Kindl, Numerical studies of finite element variational multiscale methods for turbulent flow simulations. *Comput. Methods Appl. Mech. Engrg.* **199** (2010) 841–852.
[28] V. John and W.J. Layton, Analysis of numerical errors in Large Eddy Simulation. *SIAM J. Numer. Anal.* **40** (2002) 995–1020.
[29] V. John and A. Liakos, Time dependent flow across a step: the slip with friction boundary condition. *Int. J. Numer. Methods Fluids* **50** (2006) 713–731.
[30] W. Layton, *A remark on regularity of an elliptic-elliptic singular perturbation problem*. Technical report, University of Pittsburgh (2007).
[31] W. Layton, Introduction to the numerical analysis of incompressible viscous flows. *SIAM* (2008).
[32] W. Layton, C. Manica, M. Neda and L. Rebholz, Numerical analysis and computational testing of a high-accuracy Leray-deconvolution model of turbulence. *Numer. Methods Partial Differ. Equ.* **24** (2008) 555–582.
[33] W. Layton, C. Manica, M. Neda, M.A. Olshanskii and L. Rebholz, On the accuracy of the rotation form in simulations of the Navier-Stokes equations. *J. Comput. Phys.* **228** (2009) 3433–3447.
[34] W. Layton, C. Manica, M. Neda and L. Rebholz, Numerical analysis and computational comparisons of the NS-omega and NS-alpha regularizations. *Comput. Methods Appl. Mech. Engrg.* **199** (2010) 916–931.
[35] W. Layton, L. Rebholz and M. Sussman, Energy and helicity dissipation rates of the NS-alpha and NS-alpha-deconvolution models. *IMA J. Appl. Math.* **75** (2010) 56–74.
[36] E. Lunasin, S. Kurien, M. Taylor and E.S. Titi, A study of the Navier-Stokes-alpha model for two-dimensional turbulence. *J. Turbulence* **8** (2007) 751–778.
[37] J.E. Marsden and S. Shkoller, Global well-posedness for the lagrangian averaged Navier-Stokes (lans-alpha) equations on bounded domains. *Philos. Trans. Roy. Soc. London A* **359** (2001) 14–49.
[38] G. Matthies, G. Lube and L. Roehe, Some remarks on residual-based stabilisation of inf-sup stable discretisations of the generalised Oseen problem. *Comput. Meth. Appl. Math.* **198** (2009) 368–390.
[39] W. Miles and L. Rebholz, Computing NS-alpha with greater physical accuracy and higher convergence rates. *Numer. Methods Partial Differ. Equ.* (to appear).
[40] H. Moffatt and A. Tsoniber, Helicity in laminar and turbulent flow. *Ann. Rev. Fluid Mech.* **24** (1992) 281–312.
[41] A. Muschinsky, A similarity theory of locally homogeneous and isotropic turbulence generated by a Smagorinsky-type LES. *J. Fluid Mech.* **325** (1996) 239–260.

https://doi.org/10.1051/m2an/2010042 Published online by Cambridge University Press

[42] M.A. Olshanskii, A low order Galerkin finite element method for the Navier-Stokes equations of steady incompressible flow: a stabilization issue and iterative methods. *Comp. Meth. Appl. Mech. Eng.* **191** (2002) 5515–5536.
[43] M.A. Olshanskii and A. Reusken, Grad-Div stabilization for the Stokes equations. *Math. Comput.* **73** (2004) 1699–1718.
[44] M.A. Olshanskii, G. Lube, T. Heiste and J. Löwe, Grad-div stabilization and subgrid pressure models for the incompressible Navier-Stokes equations. *Comput. Methods Appl. Mech. Engrg.* **198** (2009) 3975–3988.
[45] L. Rebholz, Conservation laws of turbulence models. *J. Math. Anal. Appl.* **326** (2007) 33–45.
[46] L. Rebholz, A family of new high order NS-alpha models arising from helicity correction in Leray turbulence models. *J. Math. Anal. Appl.* **342** (2008) 246–254.
[47] L. Rebholz and M. Sussman, On the high accuracy NS-α-deconvolution model of turbulence. *Math. Models Methods Appl. Sci.* **20** (2010) 611–633.
[48] L.R. Scott and M. Vogelius, Norm estimates for a maximum right inverse of the divergence operator in spaces of piecewise polynomials. *RAIRO Modél. Math. Anal. Numér.* **19** (1985) 111–143.
[49] S. Stolz, N. Adams and L. Kleiser, An approximate deconvolution model for large-eddy simulation with application to incompressible wall-bounded flows. *Phys. Fluids* **13** (2001) 997.
[50] P. Svaček, Application of finite element method in aeroelasticity. *J. Comput. Appl. Math.* **215** (2008) 586–594.
[51] D. Tafti, Comparison of some upwind-biased high-order formulations with a second order central-difference scheme for time integration of the incompressible Navier-Stokes equations. *Comput. Fluids* **25** (1996) 647–665.
[52] G.I. Taylor, On decay of vortices in a viscous fluid. *Phil. Mag.* **46** (1923) 671–674.

https://doi.org/10.1051/m2an/2010042 Published online by Cambridge University Press